UC Berkeley
UC Berkeley Electronic Theses and Dissertations

Title
Neural Circuits Underlying Mating Behavior in Drosophila

Permalink
https://escholarship.org/uc/item/5r99v3r6

Author
Kallman, Benjamin Rory

Publication Date
2016

Peer reviewed|Thesis/dissertation

eScholarship.org Powered by the California Digital Library
University of California

Neural Circuits Underlying Mating Behavior in *Drosophila*

By

Benjamin Rory Kallman

A dissertation submitted in partial satisfaction of the

requirements for the degree of

Doctor of Philosophy

in

Neuroscience

in the

Graduate Division

of the

University of California, Berkeley

Committee in charge:

Professor Kristin Scott, Chair
Professor Yang Dan
Professor Ehud Isacoff
Professor Iswar Hariharan

Fall 2016

ABSTRACT

Neural Circuits Underlying Mating Behavior in *Drosophila*

By

Benjamin Rory Kallman

Doctor of Philosophy in Neuroscience

University of California, Berkeley

Professor Kristin Scott, Chair

Reproduction is essential for the survival of animal species. Males and females exhibit innate sex-specific reproductive behaviors, which are established developmentally and do not require previous experience. Because mating can be energetically costly, animals have evolved mechanisms to distinguish between reproductively viable and futile conspecifics that rely largely on sex-specific pheromones. How these complex, often antagonistic cues are transmitted from the periphery to the higher brain, the neural circuits they activate, or the computational principles by which they are integrated remain unclear.

In the first part of this dissertation, I investigate the neural circuits underlying mating behavior in the fruit fly *Drosophila melanogaster,* leading to a novel model of decision-making. I employ anatomical, calcium-imaging, optogenetic, and behavioral studies to demonstrate that sensory neurons that detect female pheromones, but not male pheromones, activate a novel class of neurons in the ventral nerve cord to cause activation of P1 neurons, male-specific command neurons that trigger courtship. In addition, I show that sensory neurons that detect male pheromones, as well as those that detect female pheromones, activate GABAergic mAL neurons to inhibit P1 neurons. These data support a model in which the balance of excitatory and inhibitory inputs onto central courtship-promoting neurons regulates the decision to court.

In the second part of this dissertation, I develop methods to visualize the morphology of neurons in taste processing in the fly brain. I employ large-scale calcium imaging coupled to cell labeling to identify sweet- or bitter-responsive neurons in the subesophageal zone (SEZ), the primary taste relay in the fly brain. I successfully use this approach to label SEZ motor neurons and demonstrate that they are tuned to a single taste modality, arguing for labeled-line processing of taste from sensory input to motor output. Nonetheless, reliably labeling single, non-motor SEZ neurons using this strategy has been difficult. Using a modified approach incorporating a nuclear-localized calcium indicator, I reproducibly label a cluster of putative bitter-responsive SEZ neurons. Based on their morphology, these neurons appear to be inhibitory olfactory projection neurons (iPNs), which transmit information from the antennal lobe to the lateral horn, suggesting that taste inputs may modulate the processing of odors.

TABLE OF CONTENTS

Chapter 1
Introduction 1

Chapter 2
Excitation and inhibition onto central courtship neurons biases *Drosophila* mate choice
- Summary 13
- Introduction 14
- Results 16
- Conclusions 20
- Acknowledgements 21
- Methods 22
- Figures 27

Chapter 3
Optical methods to label taste-responsive neurons in the *Drosophila* brain
- Summary 39
- Introduction 40
- Results 42
- Conclusions 44
- Methods 45
- Figures 47

Chapter 4
Discussion 51

References 55

CHAPTER 1

Introduction

Mating as an essential innate behavior

Innate behaviors are critical for the survival of individual animals and of animal species. These include such disparate behaviors as a honeybee performing a waggle dance and a child withdrawing her hand from a hot stove. Innate behaviors are generally categorized as fixed-action patterns, developmentally programmed behavioral sequences elicited by specific "sign stimuli," an idea that was formalized by Tinbergen and Lorenz in the mid-20th century. These behaviors do not require learning or experience; their full expression depends only on being "released" by appropriate sensory input. For example, Tinbergen demonstrated that young herring gull chicks will peck at their parents' beaks to obtain food and that the sign stimulus for this behavior is the presence of a red spot in a certain position on the beak (Tinbergen and Perdeck 1950).

Mating behaviors are innate and sex-specific. Tinbergen showed that male, but not female, stickleback fish court simple fish-shaped models with swollen bellies (a feature of receptive females) but are aggressive toward models with red bellies (a male-specific feature), demonstrating that belly size and color are the relevant cues detected by males that elicit aggressive or mating behaviors (Tinbergen 1952). This sort of sex-specific behavior can be observed in all sexually reproducing species and impact the reproductive success of individual animals. These behaviors have their basis in both internal genetic and anatomical dimorphisms as well as differences in the response to external cues. As males and females of most species exhibit radically different mating behaviors, the study of mating behavior provides a window into how the central nervous system interprets particular ethologically relevant sensory stimuli. Importantly, it also provides a framework to understand how molecular-, cellular- and circuit-level differences directly lead to different behavioral responses to the same sensory stimulus. Studies in mammals and in invertebrates have begun to elucidate the mechanisms that generate sex-specific behavior.

Circuits for mating in mammals

In rodents, a host of evidence has demonstrated that the sex-specific nature of mating behaviors is due to differences in the genetic landscape and neuroanatomical structure of the central nervous system, which are established by the action of sex steroid hormones during a critical period in development. These hormones, which include estrogen and testosterone, are able to cross cell membranes and, through binding to their nuclear receptors, regulate the transcription of target genes. In adulthood, these same sex hormones are responsible for activating relevant sex-specific behaviors (Wu and Shah 2011).

Much research has focused on the role of these hormones in specifying male-typical behavior. The full repertoire of behaviors exhibited by males relies on the presence of specific sex steroid hormones at different times during an animal's life (Wu and Shah 2011). There is strong evidence to support the idea that estrogen is uniquely necessary and sufficient for the masculinization of the brain during development. While the concentration of estrogen in the male circulation is extremely low, testosterone—whose concentration surges around the time of birth in mice—can be converted to estrogen by the enzyme aromatase. Aromatase is expressed in a small, sexually dimorphic subset of neurons in the brain (Wu et al. 2009), and male mice lacking aromatase expression exhibit severe defects in mating and aggression (K. Toda, Saibara, et al. 2001; K. Toda, Okada T, et al. 2001). Similar deficits are observed in males lacking estrogen receptors (Ogawa et al. 1997). Furthermore, injecting neonatal female mice with estrogen

masculinizes their nervous system and causes them to exhibit male-typical behaviors as adults, though at lower levels than those observed in male mice (Wu et al. 2009).

In contrast to estrogen, testosterone signaling through the androgen receptor (AR) does not appear necessary to masculinize the brain during development, but does appear essential for the expression of male-typical behaviors at a wild-type level in adulthood (Wu et al. 2009; Juntti et al. 2010). AR expression is extremely sparse during the neonatal period when aromatase and ER expression is high, suggesting that AR signaling is dispensable during this time. Indeed, the normal pattern of AR expression is established several days after the concentration of circulating testosterone peaks, and this pattern depends on the presence of estrogen but not AR. Male mice with a nervous-system-specific deletion of AR show normal male-typical behaviors, but with significantly reduced frequency and intensity (Juntti et al. 2010). These data suggest that testosterone signaling is not required for the organization of male-like behaviors, but does affect the extent to which these behaviors are exhibited in adulthood.

Ongoing work aims to identify the brain regions and cell types that are important for sex-specific behaviors. One principle that has emerged from these studies is that the same molecularly defined population of neurons in both sexes—for example, those that express aromatase or a sex-steroid receptor—can produce sexually dimorphic behavior, likely through sex differences in gene expression or circuit architecture. For example, a subset of neurons in the ventrolateral compartment of the ventromedial hypothalamus (VMHvl) express the progesterone receptor (PR) and are sexually dimorphic in both number and projection target. Moreover, they control different behaviors in the two sexes: in females, PR-positive VMHvl neurons are required for sexual receptivity, while the corresponding population in males is important for both mating behavior and aggression (Yang et al. 2013). In another example, cell-specific ablation studies have shown that aromatase-expressing neurons in the medial amygdala (MeA) are required in males for intermale aggression and in females for maternal aggression, while being dispensable for mating behaviors (Unger et al. 2015), again demonstrating that the same genetically defined group of neurons promote sex-specific but related behaviors.

The role of pheromones in mammalian mating behaviors

While it is clear that sex steroid hormones play a crucial role in organizing and activating the neural circuits underlying sex-specific behaviors, external cues—namely pheromones—are arguably equally important in triggering these behaviors. Pheromones are chemical cues released and detected by members of the same species. The role of pheromones is twofold: to induce proper mating behavior and to suppress improper mating behavior. Recent studies have shown that males and females release a variety of pheromones and that sex and physiological state influence both the set of pheromones that a particular animal emits as well as the particular behaviors that a given sex pheromone activates in a recipient animal.

Similar to their role in establishing dimorphisms in the nervous system, sex-steroid hormones also shape the pheromone profile of individual animals in a sex-dependent manner. Many pheromones are synthesized directly from circulating estrogen or testosterone, suggesting a means by which the sex and reproductive state of an animal can directly affect the pheromones it emits (Stowers and Liberles 2016; Fu et al. 2015). For example, 17β-diol-disulfate, a sulfated estrogen, is released by estrous females and acts via the VNO to promote mating behavior (Haga-Yamanaka et al. 2014). In addition, indirect influences of sex steroids underlie the sex-specific synthesis of other pheromones, particularly those found in urine or lacrimal secretions. One important example of this is the sexually dimorphic synthesis of major urinary proteins

(MUPs) in the liver, a process that is dependent on testosterone. Several male-enriched MUPs are strongly attractive to females, while other MUPs promote male-male aggression (Roberts et al. 2010; Chamero et al. 2007).

On the receiving end, the sensory receptors and neurons that detect mammalian pheromones have in the last decade been relatively well characterized. In mice, pheromones are detected by vomeronasal sensory neurons (VSNs), located in the vomeronasal organ (VNO), and olfactory sensory neurons (OSNs), located in the main olfactory epithelium (MOE). VSNs and OSNs express vomeronasal receptors (VRs) and odorant receptors (ORs), respectively. Because these two classes of sensory receptors use distinct signaling mechanisms involving different target ion channels (Dulac and Torello 2003), it has been possible to independently genetically manipulate the two classes of pheromone-sensing neurons.

Genetic deletion of *Trpc2*, which is required for VSN responses, results in male and female mice that attempt to mate with mice of either sex. *Trpc2*-deficient males also show significantly decreased aggression toward other males. This suggests that, in males, VNO pheromone inputs are important both for promoting aggression and suppressing inappropriate mating toward males. In females, VNO inputs appear to both suppress male-typical behavior and activate female-typical behavior. Another striking implication from behavior of *Trpc2* mutant females is that the neural circuits for male mating behaviors are present in females, but that the absence of testosterone likely prevents their activation. This is in line with older experiments showing that treating females with testosterone can induce male sexual behavior (Manoli et al. 2013). Importantly, the MOE also appears to be essential for normal male-typical behavior. Male mice lacking *Cnga2*, a critical component of signal transduction in OSNs, exhibit significant deficits in mating and aggressive behavior.

The mammalian literature thus supports the idea that sexual dimorphisms in the nervous system are established during development and underlie sex-specific behaviors that are triggered by specific pheromonal stimuli. Nonetheless, at present only large, potentially heterogeneous brain areas have been implicated in controlling these behaviors, and how these brain areas are connected into circuits remains unknown. It is also unclear how the nervous system integrates diverse pheromonal cues to produce a coherent decision to mate or not to mate. The fruit fly *Drosophila melanogaster* provides a useful model system with which to further investigate these questions. Its behaviors are relatively easy to measure and quantify and it comes with an extensive genetic and molecular toolbox that can be used to interrogate the function of specific neuronal classes. Importantly, many of the same principles with regard to mammalian sex-specific behavior have analogues in *Drosophila*, including genetic control of sexual dimorphism and a central role for pheromones in mating.

Courtship behavior in *Drosophila*

Like mammals, *Drosophila* males attempt to mate with receptive females and not other males. The stereotyped series of actions that leads to mating is referred to as courtship and has been investigated vigorously since the first studies by Alfred Sturtevant in the early 1900's. When a male detects a potential mate, he orients toward it and then follows it for a time before tapping its abdomen with his foreleg. If the target is a receptive, conspecific female, he will pursue her while extending one wing and vibrating it to produce courtship "song." This song consists of short, rapid pulses of high frequency (termed pulse song) and longer, humming-like bouts (termed sine song) (Coen and Murthy 2016). These steps are repeated for a minute or more, after which the male extends his proboscis and applies it to the female's genitalia

("licking"). He may then attempt to mount the female several times until successful copulation takes place (Sokolowski 2001).

The complexity of this behavioral sequence means that it can be energetically costly to perform. Thus, it benefits males to direct courtship toward appropriate targets while ignoring inappropriate ones. In this way, the ability to distinguish males from females is the first and most important step in selecting among potential mates. As in mammals, the ability of a male to direct courtship towards reproductively viable targets—and away from reproductively futile ones—depends both on detection of relevant pheromonal stimuli and a masculinized nervous system to translate those stimuli into appropriate behavior.

The role of the sex-determination hierarchy and *fruitless* in courtship behavior

Differences in male and female anatomy and behavior are established during development and are under the control of the sex determination pathway. In *Drosophila*, X-chromosome number is relayed through gene regulatory networks such that each cell makes a binary choice to be either female (two X chromosomes) or male (one X chromosome) (Salz and Erickson 2010). Studies in the 1970s took advantage of this dichotomy to generate sex mosaics, in which some parts of a male's nervous system were feminized via the loss of an X chromosome in an otherwise XX fly (Kankel and Hall 1976). This strategy allowed for the pinpointing of different aspects of male courtship behaviors to different brain regions. For example, song production was mapped in this way to the ventral nerve cord, analogous to the vertebrate spinal cord (von Schlicher and Hall 1979).

Other studies, occurring more or less simultaneously with the sex-mosaic studies, further refined our understanding of the sex-determination hierarchy. The gene *Sex-lethal* (*Sxl*) was found to be an immediate and crucial target of the chromosome-counting mechanism (Cline 1978). In XX animals, *Sxl* is turned on and results in female fates. In XY animals, *Sxl* remains off and male fates are adopted (Penalva and Sánchez 2003). *Sxl* is an RNA-binding protein that regulates the processing of mRNA of the gene *transformer* (*tra*). In XX animals, *tra* mRNA is spliced such that a functional protein is produced, whereas in XY animals lacking *Sxl*, *tra* is spliced by default to produce a non-functional protein (Billeter et al. 2006).

Tra is also an RNA-binding protein. Two downstream targets of *tra* that are crucial for programming sex fate are *doublesex* (*dsx*) and *fruitless* (*fru*), both of which encode transcription factors that are expressed in the central nervous system of larval and adult flies (Yamamoto, Sato, and Koganezawa 2014). *Dsx* mutations generally affect male or female anatomy whereas *fru* mutations generally affect male-typical behaviors. Nonetheless, a recent study suggested that *dsx* may play an important role in specifying the neural circuitry underlying inter-male aggression (Koganezawa, Kimura, and Yamamoto 2016). In addition, there is evidence that both *dsx* and *fru* are required for normal male-typical morphology of some cell types (Kimura et al. 2008).

Both *dsx* and *fru* are alternatively spliced such that there are unique male- and female-specific proteins (Dsx^F or Dsx^M) or only a male-specific protein (Fru^M). Several experiments suggest that Fru^M expression is critical for proper male-typical courtship behaviors. Males lacking Fru^M show severe defects in courtship of females, and females with ectopic expression of Fru^M exhibit most of the behaviors typical of male courtship, though with decreased robustness (Demir and Dickson 2005). Thus, Fru^M appears to be both necessary and sufficient for male-typical behavior. Evidence from several studies has suggested that Fru^M exerts its effects by controlling the development of sexually dimorphic neural circuits, analogous to the

masculinizing role of estrogen in the central nervous of male mice. The generation of a *fru*-Gal4 line allowed for visualization of *fru* expression in both males and females and for manipulation of *fru*-expressing neurons to test their role in courtship behavior. *Fru* was shown to be expressed in both peripheral and central neurons in a sexually dimorphic manner, with more *fru* neurons in males than females (Manoli et al. 2005; Stockinger et al. 2005). Silencing all *fru*-expressing neurons caused a robust decrease in male courtship behavior toward females, demonstrating that the activity of *fru* neurons as a whole is critical for courtship behavior (Stockinger et al. 2005). Later studies characterized individual *fru*-expressing neuronal classes and found that many were sexually dimorphic in morphology and number, and that male-specific morphology was dependent on expression of Fru^M in males (Cachero et al. 2010b; Yu et al. 2010; Datta et al. 2008).

Sensory cues that trigger courtship

Intriguingly, many *fru*-expressing neurons overlapped extensively in the male brain, suggesting that Fru^M may mark neural circuits that underlie courtship, perhaps from sensory input to motor output. In line with this, triggering courtship behavior requires the detection of specific external cues by peripheral sensory organs, many of which express *fru* (Stockinger et al. 2005). While integration of information from multiple senses—namely vision, taste, and smell—is necessary for the production of a full courtship sequence (Krstic, Boll, and Noll 2009), vision in particular is essential for determining whether to approach a moving target and to initiate courtship. A recent study that used fly "dummies" of varying sizes and shapes moving at different speeds demonstrated that male flies preferentially initiate courtship when paired with dummies of approximately the same dimensions as a *Drosophila melanogaster* female (Agrawal, Safarik, and Dickinson 2014).

In contrast, when assessing the sexual identity of a potential mate, flies appear to rely most heavily on sex pheromones. Males and females have distinct, sex-specific pheromonal profiles (Billeter et al. 2009), suggesting that pheromones could be used by a courting male to determine the sex of a target fly. In the study mentioned above, perfuming appropriately sized dummy flies with female pheromones did not influence courtship initiation but did lengthen the amount of time spent courting. Conversely, perfuming a dummy with male pheromones strongly suppressed both courtship initiation and duration (Agrawal, Safarik, and Dickinson 2014). These results suggest that male flies use visual cues to identify an active fly-sized target, but that detection of female-enriched, aphrodisiac pheromones is also necessary to promote and maintain vigorous courtship. In addition, these data show that male-enriched, anti-aphrodisiac pheromones are detected before physical contact and are sufficient to block courtship initiation.

Sex pheromones fall broadly into two categories: volatile (long-range) pheromones and non-volatile (contact) pheromones, which are sensed by the olfactory and gustatory systems, respectively. The identity of some of these courtship-promoting and -inhibiting pheromones has been known for several decades. The best-studied volatile pheromone is *cis*-vaccenyl acetate (cVA), which is synthesized in the male ejaculatory bulb and transferred to females upon mating. In males, cVA acts through the olfactory receptor Or67d to suppress courtship toward previously mated females and also acutely to trigger male-male aggression (Kurtovic, Widmer, and Dickson 2007; L. Wang and Anderson 2010). Male flies mutant for the Or67d gene show increased levels of inappropriate male-male courtship and, unlike controls, do not exhibit lower courtship levels toward females treated with cVA. Interestingly, chronic cVA exposure has been shown to suppress male-male aggression via the Or65a receptor (Liu et al. 2011). In females, cVA enhances receptivity (Kurtovic, Widmer, and Dickson 2007), demonstrating that the same

pheromone can induce different behaviors in males and females. Beyond cVA, no other volatile pheromones had been conclusively identified until a recent study characterized several courtship-promoting pheromones. These include methyl laurate, methyl myristate, and methyl palmitate, which are detected by Or47b- and Or88a-expressing ORNs (Dweck et al. 2015).

In addition, Ir84a, a member of the ionotropic receptor (IR) superfamily, has been shown to be important for courtship behavior. Ir84a-expressing ORNs do not respond to male or female pheromonal extracts but, surprisingly, are strongly activated by phenylacetic acid and phenylacetaldehyde, two aromatic odors found in fruit. Ir84a mutant males court females, but they do so with about half the robustness of control males, suggesting that the detection of aromatic fruit odors is required for maximal levels of courtship. Indeed, the presence of phenylacetic acid or normal fly food enhanced courtship toward a decapitated female—a target that normally elicits low levels of courtship from wild-type males—in an Ir84a-dependent manner (Grosjean et al. 2011). Thus, the neural circuits activated by Ir84a-expressing ORN appear to couple the presence of food with mating behavior and suggest that food odors serve a role complementary to fly-derived pheromones in promoting courtship.

Notably, Or67d-, Or47b-, and Ir84a-expressing ORNs all co-express *fruitless*. They send their axons to the DA1, VA1v, and VL2a glomeruli, respectively, all of which are sexually dimorphic (i.e. larger in males than in females) (Manoli et al. 2005; Stockinger et al. 2005). While responses of Or67d-expressing ORNs to cVA are not different between the sexes, the neural circuit downstream of these cells has been shown to be sexually dimorphic (Datta et al. 2008; Ruta et al. 2010; Kohl et al. 2013). First, the axons of DA1 projection neurons (PNs) were shown to have a male-specific ventral projection in the lateral horn, their target brain region. This anatomical dimorphism underlies differential connections between DA1 PNs and their synaptic partners. In males, the axonal termini of DA1 PNs overlap with third-order aSP-f neurons (also known as DC1), whereas in females, DA1 PN axons overlap with aSP-g neurons. As predicted anatomically, aSP-f neurons respond to cVA in males (but not females) while aSP-g neurons respond to cVA in females (but not males). This bidirectional circuit switch suggests an anatomical means by which the same pheromone can elicit different behaviors in males and females. Each level of the cVA circuit—first-, second-, and third-order neurons—all express Fru^M, which is required for male-typical anatomy and functional responses, providing further evidence to suggest that Fru^M is a marker for neurons involved in courtship.

While the cVA circuit has been elegantly dissected, cVA is just one cue used by male flies to distinguish between the sexes. Arguably as important are contact pheromones. These are principally long-chain cuticular hydrocarbons (CHCs), which are synthesized in specialized abdominal cells called oenocytes and are deposited on the cuticle. Males and females have distinct, sex-specific CHC profiles. Males are enriched in CHCs with one double bond, such as 7-tricosene (7-T) and 7-pentacosene (7-P), while females are enriched in CHCs with two double bonds, such as 7,11-nonacosadiene (7,11-ND) and 7,11-heptacosadiene (7,11-HD) (Ferveur 2005). 7-T has been shown to inhibit male courtship toward females, while 7,11-HD and 7,11-ND have been shown to enhance it (Billeter et al. 2009). Male and female flies lacking CHCs (due to genetic ablation of oenocytes) elicit roughly equal levels of courtship from wild-type males, suggesting that oenocyte-derived CHCs impose sexual identity onto a weakly attractive fly substrate. In line with this, perfuming oenocyte-ablated (oe-) flies with male CHCs inhibits courtship whereas perfuming them with female CHCs promotes courtship (Billeter et al. 2009; Agrawal, Safarik, and Dickinson 2014; Thistle et al. 2012).

CHCs are detected mainly by gustatory receptor neurons (GRNs) on the legs. A handful of sensory receptors that are expressed in leg GRNs have been implicated in pheromone detection. Male flies mutant for the gustatory receptors Gr32a or Gr33a exhibited high levels of aberrant male-male courtship, suggesting that these receptors detect an inhibitory contact pheromone (Miyamoto and Amrein 2008; Moon et al. 2009). Flies lacking Gr32a were shown to be insensitive to the courtship-inhibiting effect of 7-T, arguing the Gr32a is a receptor for 7-T (L. Wang et al. 2011). Nonetheless, this hypothesis has not been directly tested with functional assays. Interestingly, unlike in controls, synthetic cVA does not promote aggression in Gr32a mutant males, suggesting a hierarchy in which male-enriched CHCs like 7-T gate the aggression-promoting effect of cVA. This appears to be independent of cVA's courtship-suppressing effect, as the courtship of Gr32a mutant and control males toward females is equally inhibited by cVA (L. Wang et al. 2011).

The role of another GR, Gr68a, has been more controversial. One study found that silencing Gr68a-expressing neurons with tetanus toxin lowered both wing extension rate and copulation success. Male flies in which Gr68a expression was knocked down in Gr68a-expressing cells via RNAi exhibited similar defects in courtship. Gr68a was found to be expressed in chemosensory neurons in the forelegs of male flies, but, interestingly, no expression was observed in females. These data suggested that Gr68a was a male-specific receptor for a courtship-promoting cuticular pheromone (Bray and Amrein 2003). However, a later study observed that Gr68a was also expressed in tissues other than the foreleg, including the antenna and proboscis. In these organs, Gr68a appeared to label mechanosensory and auditory neurons. The courtship level of males in which Gr68a-expressing neurons were silenced depended on the size of the chamber used for the courtship tests: in small chambers, Gr68a-silenced males exhibited normal levels of courtship, but in larger chambers these males had deficits in courtship initiation and maintenance, suggesting that Gr68a functions both before and during male-female contact. The authors suggest that acoustic or vibratory signals are detected by Gr68a-expressing mechanosensory neurons before a male "finds" a female, and that the activity of Gr68a-expressing GRNs are required for maintenance of robust courtship after initiation (Ejima and Griffith 2008). Deciphering the exact role of gustatory versus mechanosensory Gr68a-expressing neurons in courtship behavior will depend on the generation of genetic tools that label each subtype independently.

More recently, two related members of the IR superfamily, Ir52c and Ir52d, were found to be expressed in subset of foreleg GRNs in a sexually dimorphic manner. These leg GRNs responded with calcium increases to the presence of virgin females, and male flies mutant for Ir52c or Ir52d exhibited deficits in female-directed courtship. Specifically, mutant males had a prolonged latency to court (i.e. time to first unilateral wing extension) and took longer to achieve copulation (Koh et al. 2014), suggesting that Ir52c and Ir52d detect one or more courtship-promoting pheromones, although this as not tested directly.

Intriguingly, most leg taste bristles house two *fruitless*-positive GRNs that send axons into the ventral nerve cord (VNC). The projection pattern of these axons is sexually dimorphic: male axons cross the midline while female axons remain unilateral (Mellert et al. 2010). The fact that cVA-responsive ORNs also express *fruitless* suggests that these leg GRNs might sense contact pheromones. While none of the GRs or IRs discussed above appear to be expressed in the *fru*-positive GRNs, our lab and others recently identified two previously uncharacterized genes, *pickpocket 23* (*ppk23*) and *pickpocket 25* (*ppk25*), which are co-expressed in the *fru*-positive leg GRNs. Both genes encode ion channel subunits within the degenerin/epithelial

sodium channel family that had no known function (Thistle et al. 2012; H. Toda, Zhao, and Dickson 2012; Lu et al. 2012; Starostina et al. 2012).

Male flies mutant for *ppk23* exhibit increased male-male courtship and decreased courtship toward females, a phenotype resembling that of *fru* mutants. Silencing PPK23-positive neurons with tetanus toxin, which blocks neurotransmission, also leads to increased male-male and decreased male-female courtship. Males in which PPK23 cells are activated using dTRPA1, a temperature-sensitive cation channel, show decreased courtship towards normally attractive oe- male flies, but increased courtship toward oe- female flies, demonstrating a courtship target-specific effect of PPK23 cell activation. *Ppk23* mutants are also insensitive to the behavioral effects of CHCs: control males reduce courtship toward oe- males that are perfumed with 7-T or 7-P, whereas *ppk23* mutants do not. Similarly, perfuming oe- females with aphrodisiac 7,11-HD or 7,11-ND elicits more robust courtship from control but not *ppk23* mutant males (Thistle et al. 2012).

Taken together, these behavioral results suggest that the leg GRNs that co-express PPK23 and *fruitless* detect contact pheromones in a PPK23-dependent manner. This was confirmed by monitoring the response of PPK23 cells to pheromones with the genetically encoded calcium indicator G-CaMP. Interestingly, one of the two PPK23 cells responded specifically to male CHCs (hereafter the M cell), while the other responded specifically to female CHCs (hereafter the F cell). In subsequent experiments, it was shown that PPK25 is expressed in one of the two PPK23 cells under each bristle and that it is required for the response to female but not male pheromones, suggesting that PPK25 is expressed in F cells (Vijayan et al. 2014). F and M cells are present in both sexes, but they are more numerous in males. In addition, F and M cells extend sexually dimorphic projections. In male flies, their axons cross the midline of the VNC whereas in females they do not. The role of F and M cells in female mating behavior remains unknown.

In summary, the sensory receptors that detect pheromones, and the peripheral neurons in which they are expressed, have been relatively well studied, with PPK23 cells in particular appearing crucial for both promoting robust courtship toward females and suppressing inappropriate courtship toward males.

Pheromone-responsive neural circuits in the central brain

Significantly less is known about the central neural circuits in the male brain that are activated by cuticular pheromones. Using intersectional genetic techniques, several anatomical studies have mapped *fru*-expressing neuronal clusters onto a common brain, providing a cellular-level description of the neurons that likely comprise the courtship circuit and allowing for the drawing of potential connections between different clusters.

Of the more than 100 distinct *fru*-expressing neuronal classes (Yu et al. 2010), one cluster of approximately 30 male-specific neurons in the posterior brain—the P1 neurons—has been proposed to be a critical node within the courtship circuit and appears to be both necessary and sufficient for robust courtship. Evidence for the sufficiency of P1 neurons in producing courtship behavior comes from one study that used the mosaic analysis technique MARCM to generate subsets of neurons in the female brain that were mutant for the sex-determination gene *transformer*, thus masculinizing them. In this way, it was possible able to correlate abnormal, male-typical behavior in females with the masculinization of particular cell types. These experiments demonstrated that the presence of P1 neurons in the female brain was correlated with high levels of male-typical courtship behavior, including orientation, tapping, following, and wing extension. Furthermore, P1 neurons were shown to co-express *fruitless* and *doublesex*.

Dsx^F was found to be required for the normal apoptotic elimination of P1 neurons in female brains, such that females lacking Dsx^F possessed ectopic P1 neurons. Importantly, males lacking either Fru^M or Dsx^M retained P1 neurons, but they were fewer in number and had abnormal morphology. This was suggested to explain the previously observed diminished courtship of *fru* mutant males (Kimura et al. 2008; Kimura et al. 2005). Taken together, these data show that Dsx^F is required in females to eliminate P1 neurons and suppress male courtship behavior, and suggest that both Dsx^M and Fru^M are required in males for normal P1 neuron morphology and courtship behavior.

Two later studies tested more directly the link between P1 neuron activity and courtship behavior. Using intersectional genetic approaches that enable the visualization and manipulation of specific *fru*-expressing neuronal classes, these studies undertook thermogenetic activation screens with the goal of identifying neurons important for courtship behavior. By expressing dTRPA1 in specific *fru*-expressing classes, it was shown that heat-induced activation of P1 neurons was sufficient to induce many aspects of courtship behavior in isolated males, including tapping, licking, wing extension, and the pulse component of courtship song. In contrast, males in which tetanus toxin was expressed in P1 neurons displayed greatly reduced courtship song and copulated much less frequently than control males (von Philipsborn et al. 2011; Kohatsu, Koganezawa, and Yamamoto 2011). Importantly, one of these studies took the additional step of testing whether P1 neurons are activated by pheromonal cues. Using calcium imaging, Kohatsu and colleagues demonstrated that P1 neurons are excited by female pheromones and, to a lesser extent, male pheromones. They also demonstrated that the response in P1 neurons to female pheromones is blunted by co-presentation of cVA. Thus, P1 neurons appear to be central courtship-promoting neurons, but the neural pathways that transmit pheromonal information to P1 neurons have not been described.

Another class of Fru neurons that has been studied relatively extensively is the mAL neurons (also known as aDT2). mAL neurons are sexually dimorphic in both number and morphology. In males, approximately 30 mAL neurons have cell bodies dorsal to the antennal lobes and extend contralateral projections that arborize in both the SEZ (in a "horse-tail" shape) and the protocerebrum. In females, about five mAL neurons have similar cell body locations, but they arborize in a Y-shape in the SEZ and project to a more lateral region of the protocerebrum. Importantly, the male-typical morphology of mAL neurons requires Fru^M; in its absence mAL neurons are reduced to approximately the same number as found in females and have female-like morphology (Kimura et al. 2005).

There is limited evidence that, in male flies, mAL neurons may receive pheromonal input and modulate courtship behavior. mAL arborizations in the SEZ overlap with incoming axons from the legs, suggesting that mAL neurons may be downstream of leg pheromone-sensing cells. Manipulating mAL neurons using the intersectional genetic approaches discussed above uncovered a correlation between mAL silencing and improper wing extension. Male flies with silenced mAL neurons exhibited a significantly increased rate of simultaneous wing extension, as compared to control flies, which normally only extend one wing at a time. This same phenotype was observed in flies with silenced Gr32a-expressing neurons, suggesting that mAL neurons may received input from these cells to regulate unilateral wing extension (Koganezawa et al. 2009)

Thus, while much progress has been made in identifying the environmental cues that either promote or inhibit *Drosophila* mating behaviors—as well as the sensory receptors and neurons that detect these cues—the neural circuits that underlie appropriate courtship are

incompletely understood. A few *fruitless*-positive clusters have been shown to be involved in regulating courtship behavior and potentially receive pheromonal inputs, but the specific sensory neurons that detect these cues, and the neural pathways conveying this pheromonal information from the periphery are unknown. Chapter 2 of this thesis uncovers sensory pathways in the male CNS that transmit the detection of courtship-promoting or courtship-suppressing pheromones to *fruitless*-expressing neurons in the higher brain. These pathways either excite or inhibit a male-specific class of neurons that promotes courtship, suggesting a model in which a group of central integrative neurons weighs multiple, potentially antagonistic sensory inputs to produce a singular decision to mate.

Developing techniques to dissect other sensory circuits

Fruitless expression has allowed researchers to identify and test the role of candidate neurons in courtship behavior, but such a convenient molecular tag has not been identified—and possibly does not exist—for other sensorimotor circuits. Central circuits downstream of gustatory receptors neurons (GRNs) have been especially resistant to anatomical or functional characterization. GRNs that detect different taste modalities project to different, but relatively diffuse, regions in the subesophageal zone (SEZ) of the brain. Unlike the antennal lobe, which is dedicated to the processing of odors, the SEZ is a multimodal region that receives inputs from several organs and also houses many descending neurons involved in motor control and grooming (Hsu and Bhandawat 2016; Hampel et al. 2015). With no clear molecular or anatomical markers, the identity of taste-responsive SEZ neurons has remained illusive. Thus, visualizing the morphology of taste-responsive SEZ neurons is a necessary first step towards understanding the computational principles and characterizing the behavioral role of taste circuits in the brain. Chapter 3 of this thesis describes a series of large-scale calcium-imaging and cell-labeling experiments carried out with this goal in mind. While several technical hurdles remain, these approaches have yielded interesting and unexpected results suggesting that taste may affect the processing of odors.

CHAPTER 2

Excitation and inhibition onto central courtship neurons biases *Drosophila* mate choice

Summary

The ability to distinguish males from females is essential for productive mate selection and species propagation. Recent studies in *Drosophila* have identified different classes of contact chemosensory neurons that detect female or male pheromones and influence courtship decisions. Here, we examine central neural pathways in the male brain that process female and male pheromones. Using anatomical, calcium-imaging, optogenetic, and behavioral studies, we find that sensory neurons that detect female pheromones, but not male pheromones, activate a novel class of neurons in the ventral nerve cord to cause activation of P1 neurons, male-specific command neurons that trigger courtship. In addition, sensory neurons that detect male pheromones, as well as those that detect female pheromones, activate central mAL neurons to inhibit P1. These studies demonstrate that the balance of excitatory and inhibitory drives onto central courtship-promoting neurons controls mating decisions.

This work has been previously published:

Kallman, B.R., Kim, H., Scott K (2015). Excitation and inhibition onto central courtship neurons biases mate choice. *eLife* 4: e11188.

Introduction

Across the animal kingdom, the ability to distinguish males from females is critical to select among potential mates. The specificity of mating decisions is exemplified by the *Drosophila* courtship ritual, in which males follow, sing to, and copulate with females but not males. Although much progress has been made in identifying the circuits that underlie mating decisions in the male fly brain, the sensory neurons that detect sex-specific cues and the pathways that they activate to generate sex-specific behaviors are incompletely understood.

A major advance in elucidating the neural circuits that govern male mating decisions has come from the discovery that a male-specific splice form of the Fruitless transcriptional regulator (Fru^M) is expressed in peripheral and central neurons that drive courtship behavior (Manoli et al. 2005; Stockinger et al. 2005), arguing that Fru^M marks neural circuits for courtship. Studies of the function of Fru^M-positive neurons has led to the identification of olfactory and gustatory neurons that detect pheromones, as well as central neurons that drive behavioral subprograms of courtship (Ruta et al. 2010; Datta et al. 2008; Ha and Smith 2006; Thistle et al. 2012; H. Toda, Zhao, and Dickson 2012; Kurtovic, Widmer, and Dickson 2007).

One set of neurons that has emerged as a central driver of male mating behavior is the P1 (a.k.a. pMPe, pMP4 or pC1) neurons in the protocerebrum (Lee, Hall, and Park 2002; K. I. Kimura et al. 2005; Yu et al. 2010; Cachero et al. 2010). Inducible activation of these neurons leads to sustained male courtship behaviors (Inagaki et al. 2014; von Philipsborn et al. 2011; Pan, Meissner, and Baker 2012; Kohatsu, Koganezawa, and Yamamoto 2011). Moreover, these neurons are activated by female pheromones and this activation is partially inhibited in the presence of the male inhibitory pheromone, *cis*-vaccenyl acetate (cVA) (Kohatsu, Koganezawa, and Yamamoto 2011). These data show that P1 neurons receive sensory cues signaling females or males and drive courtship decisions, suggesting that they may be command neurons for courtship behaviors.

The sensory pathways that converge onto P1 neurons are poorly defined. Diverse sensory stimuli contribute to courtship decisions, including visual, auditory, and chemosensory cues. Important sensory cues detected primarily by contact chemosensory neurons are sex-specific cuticular hydrocarbons that act as pheromones. Multiple gustatory receptors and neurons have been implicated in pheromone detection (Koh et al. 2014; Watanabe et al. 2011; Moon et al. 2009; Bray and Amrein 2003; Miyamoto and Amrein 2008). We and others recently showed that leg chemosensory neurons expressing the PPK23 pickpocket ion channel detect pheromones (H. Toda, Zhao, and Dickson 2012; Lu et al. 2012; Thistle et al. 2012). PPK23 is expressed in sensory neurons of many leg chemosensory bristles, with generally two PPK23 cells per bristle. One cell responds selectively to male pheromones (M cells) and the other cell to female pheromones (F cells) (Thistle et al. 2012; Pikielny 2012; Vijayan et al. 2014). In contrast, the PPK25 channel is expressed in one of the two PPK23-positive cells per bristle, and PPK25 is required for cellular and behavioral responses to female pheromones, arguing that it selectively labels F cells (Starostina et al. 2012; Vijayan et al. 2014). Unlike other classes of gustatory neurons implicated in pheromone detection, PPK23 cells are Fruitless-positive (H. Toda, Zhao, and Dickson 2012; Lu et al. 2012; Thistle et al. 2012). This suggested that it may be possible to trace pheromonal pathways from PPK23 cells in the periphery to the central nervous system by using Fru^M neurons as a guide.

Here, we examine the sensory pathways in the male brain, from pheromone-sensing cells on the legs to the ventral nerve cord to the protocerebrum, in order to elucidate the neural circuits

underlying a male fly's ability to distinguish between appropriate and inappropriate mates. These studies define sensory pathways that act as excitatory and inhibitory drives onto P1, providing insight into the functional connectivity of the courtship circuit.

Results

Genetic access to cells that sense female or male pheromones

To examine pathways activated by female excitatory pheromones and male inhibitory pheromones, we focused on different subpopulations of PPK23 cells as specific sensory inputs. By GCaMP6s calcium imaging (T.-W. Chen et al. 2013) of PPK23 cells in a background in which PPK25 cells were independently labeled, we first confirmed that the PPK25-positive cells (F cells) are tuned to female pheromones and the PPK25-negative cells (M cells) to male pheromones (Figure 2.1A, B; Table 1 contains genotypes of flies used for all experiments). In addition, we found that F cells are the only leg neurons that express the vesicular glutamate transporter (vGlut) (Daniels et al. 2008), demonstrating that the two classes differ in their neurotransmitter profiles and providing an additional marker that selectively labels F cells (Figure 2.1C, D). F cells and M cells also differ in their axonal projection patterns: F cells terminate in the ventral nerve cord (VNC) whereas M cells also have fibers that project to the subesophageal zone (SEZ) of the central brain (Figure 2.1E, G).

To ask whether F or M cell activation is sufficient to modify courtship behavior, we used genetic strategies to express the heat-activated cation channel dTRPA1 (Hamada et al. 2008) selectively in F or M cells. A single male was placed in a chamber with a virgin female and number of single wing extensions by the male was monitored, as this motor subprogram occurs specifically during courtship song production. Males expressing dTRPA1 in F cells tested at 30°C had a significantly higher wing extension rate than genetically identical flies tested at 23°C or control flies at either temperature (Figure 2.1F). In contrast, males expressing dTRPA1 in M cells had a significantly lower wing extension rate at 30°C compared to genetic and temperature controls (Figure 2.1H). Thus, F and M cells comprise genetically and anatomically distinct chemosensory neuron classes that respond to female or male pheromones and promote or inhibit courtship.

F cell stimulation activates P1 neurons

The ability to genetically access and specifically activate cells responding to female or male pheromones provided the opportunity to trace sex-selective pathways in the male brain and examine the neural substrates for courtship decisions. We genetically accessed F cells with the *ppk25-Gal4*, *vGlut-LexA* and *vGlut-QF2* drivers, all of which specifically label F cells in the legs (Figure 2.1C, D, and 2.2A). To selectively access M cells (PPK23-positive, PPK25-negative cells), we used a driver that labels both F and M cells (*ppk23-LexA*) while driving Gal80 with F cell drivers (Figure 2.2B). The ATP-gated cation channel P2X2 (Lima and Miesenböck 2005) was selectively expressed in these sensory classes and ATP was applied to the legs for robust cell-specific activation.

Male-specific, Fru-positive P1 neurons (Cachero et al. 2010b; Yu et al. 2010; K. ichi Kimura et al. 2008; Lee, Hall, and Park 2002) are prominent courtship-promoting neurons in the protocerebrum that trigger sustained courtship behaviors upon ectopic activation (Kohatsu, Koganezawa, and Yamamoto 2011; Pan, Meissner, and Baker 2012; von Philipsborn et al. 2011; Inagaki et al. 2014). As P1 neurons have been shown to respond to hydrocarbon extracts from female and male abdomens (Kohatsu, Koganezawa, and Yamamoto 2011), we tested whether F and M cells provided specific sensory inputs onto P1 neurons. P1 activity was monitored by GCaMP6s calcium imaging in live flies expressing P2X2 in both F and M cells (F+M), F cells, or M cells while ATP was applied to the legs (Figure 2.3A, B). Activation of F cells triggered

calcium increases in P1, demonstrating that sensory neurons that detect female pheromones activate courtship-promoting P1 neurons. In contrast, we observed no significant calcium response in P1 neurons upon M cell activation. Activating F+M cells using the same *ppk23-LexA* driver (without expression of Gal80 in F cells) caused robust calcium responses in P1 neurons. These experiments argue that F cells, but not M cells, activate P1 neurons. This is in contrast to a previous study that observed calcium increases in P1 neurons in response to male abdomens (Kohatsu, Koganezawa, and Yamamoto 2011); however, male abdomens may activate other sensory neurons in addition to M cells, such as Fru-negative pheromone-sensing neurons, gustatory neurons, or mechanosensory neurons. The selective activation of single classes of sensory cells allows us to disambiguate sensory cues and determine the contribution of specific sensory inputs.

PPN1 neurons respond to F cell stimulation and activate P1 neurons

As F cells terminating in the VNC do not directly contact P1, we screened existing Gal4 collections (Gohl et al. 2011; Jenett et al. 2012) for neurons that might contact F cell projections and project to higher brain regions. We identified a pair of neurons with dendrites in the VNC and axons in the protocerebrum, which we name Pheromone Projection Neuron class 1 (PPN1) (Figure 2.4A-C). PPN1 neurons have cell bodies in the third leg neuromere, send projections to all leg and wing neuromeres in the VNC, and terminate in the ventrolateral protocerebrum. PPN1 dendrites are in close proximity to PPK23 axons and PPN1 axons overlap with P1 fibers, as shown by double labeling experiments (Figure 2.4E, F). To test whether PPN1 is involved in courtship behavior, we expressed dTRPA1 in PPN1 neurons and monitored male courtship towards females upon heat-induced neural activation. Consistent with a role in promoting courtship, activating PPN1 with dTRPA1 increased male courtship behavior toward females, as measured by unilateral wing extension rate (Figure 2.4D). Unlike other neurons of the courtship circuit, PPN1 is not Fru-positive based on intersectional approaches with *Fru-Flp* and *Fru-LexA* and PPN1 projections are not sexually dimorphic (data not shown). Nonetheless, the anatomical and behavioral studies suggest that PPN1 might transmit F cell activation to P1 to promote courtship.

To test whether PPN1 receives pheromonal signals, we stimulated F cells or M cells by ATP-mediated activation of P2X2 while monitoring calcium changes in PPN1 axons in the higher brain. These studies revealed calcium increases in PPN1 axons upon F cell stimulation but not M cell stimulation (Figure 2.5A, B). As with P1, activating F+M cells using the same *ppk23-LexA* driver (without expression of Gal80 in F cells) triggered robust calcium responses in PPN1, further arguing that PPN1 neurons are downstream of F cells and not M cells. To more directly test whether F cell activity is transmitted to P1 by PPN1, we expressed the red-shifted opsin Chrimson (Klapoetke et al. 2014) in PPN1 and monitored calcium changes in P1. Activation of PPN1 with red light generated calcium responses in P1 (Figure 2.5C, D). Red light had no effect on P1 activity in control animals not fed the essential cofactor retinal. Together, these experiments argue that female pheromones activate a neural pathway from F cells to PPN1 to P1 to drive courtship behavior.

M cells and F cells activate mAL neurons

As M cell stimulation did not activate P1, we searched for other targets of F and M cells by monitoring calcium responses in all Fru neurons upon F+M cell stimulation, observing activity throughout the brain using spinning disk confocal microscopy. One set of neurons was

prominently activated by F+M stimulation (Figure 2.6A, B). These were anatomically identifiable as mAL neurons (a.k.a. aDT2, aDTb) by their distinct arborization patterns (Kimura et al. 2005; Yu et al. 2010; Cachero et al. 2010; Ito et al. 2012). Based on their anatomy and neurotransmitter profile, mAL neurons have been proposed to be sexually dimorphic GABAergic interneurons that convey inhibitory courtship signals to the higher brain in males (Koganezawa et al. 2009) (Figure 2.7A, B). Consistent with this, we found that M cell axons and mAL dendrites overlap in the SEZ (Figure 2.7C-E). However, the behavioral role of mAL neurons in courtship, the sensory stimuli that activate mAL, and the relationship between mAL and other components of the courtship circuit have not been determined.

To test whether mAL neurons participate in courtship behavior, we conditionally activated or inactivated them using the genetic intersection of *R43D01-Gal4* and *Fru-LexA* and monitored courtship behavior. Activation of mAL neurons with dTRPA1 greatly suppressed courtship toward females compared to controls (Figure 2.6C), as measured by unilateral wing extension rate. Inactivation of mAL neurons with tetanus toxin caused robust male-male chaining, a behavior in which three or more males serially court each other (Figure 2.6D), and which was almost never observed in control animals. Furthermore, expression of RNAi against the vesicular GABA transporter (vGAT) using *R43D01-Gal4* also caused male-male chaining (Figure 2.6D), arguing that GABA release from mAL inhibits courtship. Thus, activation of mAL inhibits courtship, whereas inactivation enhances courtship, demonstrating an inhibitory role for mAL in courtship decisions.

Finally, we tested the specificity of the response of mAL neurons to pheromone sensory cell stimulation, using the *R43D01-Gal4* line to express GCaMP6s and the same drivers used for the PPN1 and P1 experiments to express P2X2 in M and F cells (Figure 2.6E, F). Surprisingly, both M cells and F cells activated mAL, arguing that detection of female as well as male pheromones provides an inhibitory courtship drive. As F cells additionally activate PPN1 and P1 courtship-promoting neurons, whereas M cells do not, this suggests that the balance between excitation and inhibition onto P1 neurons underlies the decision to court.

mAL neurons inhibit P1 courtship command neurons

How do mAL neurons inhibit courtship? P1 neurons are in close proximity to mAL termini (Figure 2.8A), suggesting that they may be candidate targets of GABAergic mAL neurons. To test whether P1 neurons receive inhibitory signals, we generated flies containing an RNAi against the $GABA_A$ receptor subunit Resistant to dieldrin (Rdl) (Ffrench-Constant et al. 1991) in P1 neurons and examined the behavioral consequence. Males expressing Rdl RNAi in P1 neurons displayed increased courtship toward other males, arguing that P1 neurons receive GABAergic inhibition (Figure 2.8B). In addition, whereas Chrimson-mediated activation of P1 neurons induced courtship behavior in solitary males, co-activation of P1 and *R43D01-Gal4* neurons suppressed this behavior (Figure 2.8C), arguing that mAL suppresses P1-mediated courtship. To more directly test whether inhibitory signals from mAL impinge on P1, we simultaneously stimulated F and M cells and monitored activity in P1 before and after two-photon guided lesioning of mAL axons (Figure 2.8D, 2.7F). Indeed, simultaneous stimulation of F and M cells caused transient activation of P1 and lesioning mAL axons significantly increased P1 activation.

These data suggest that mAL neurons inhibit P1 neurons via $GABA_A$ receptors. To test directly whether mAL input onto P1 causes hyperpolarization, we expressed ArcLight (Cao et al. 2013), a fluorescent voltage sensor, in P1 neurons and monitored its fluorescence using two-

photon imaging (Figure 2.8E). Chrimson-mediated activation of mAL neurons, using *R43D01-LexA* (Figure 2.7G), evoked a rapid increase in ArcLight fluorescence in P1 neurons, indicating hyperpolarization. No fluorescence change was observed in control flies lacking the *R43D01-LexA* transgene. These experiments demonstrate that mAL neurons provide an inhibitory drive onto P1 neurons.

Conclusions

This work identifies pheromone-responsive neural circuits underlying mating decisions. We used cell-specific activation to determine sensory pathways that impinge on courtship-promoting P1 neurons, providing insight into the functional connectivity of the courtship circuit. Female pheromones trigger neural pathways that excite and inhibit P1, with PPN1 providing an excitatory drive onto P1 and mAL providing an inhibitory drive. F cell activation leads to P1 activation and increased courtship behavior, arguing that the sum of inputs onto P1 produces excitation or that the sequence of inputs, i.e., fast excitation followed by inhibition, provides a temporal window for excitation. In contrast, M cells activate mAL neurons to inhibit P1 and inhibit courtship behavior. These studies argue that the balance of excitation and inhibition onto P1 neurons is different following F cell or M cell activation: F cell activation leads to overall P1 activation whereas M cell activation leads to overall P1 inhibition.

Our calcium imaging studies provide strong support that the pathways identified in this study are activated by F and M cell stimulation, and our behavioral experiments demonstrate that activation of these neurons directly contributes to courtship decisions. However, we do not exclude the possibility that additional intermediary neurons may also be activated by F or M cells. Indeed, a recent study identified vAB3 neurons, which project from the first leg neuromere in the VNC to the SEZ and protocerebrum, as being activated by female but not male pheromones (Clowney et al. 2015). This study also showed that mAL neurons are activated by male and female abdomens and provided evidence that mAL inhibits P1. Our independent observations are consistent with this work and extend the findings by providing behavioral evidence that each identified component of the circuit promotes or inhibits courtship as predicted by its response properties, by using cell-type-specific activation strategies coupled with cell-type-specific imaging studies to directly test potential connections, and by identifying PPN1 as a novel neural component of the courtship circuit. Together, the studies argue that pheromones activate multiple excitatory and inhibitory interneurons that impinge on P1.

A caveat of our studies is that they rely on ectopic expression of reporters, and expression levels of P2X2 and GCaMP6s may influence the ability to detect responding cells. Nevertheless, the same driver was used to express P2X2 in M cells in all calcium-imaging experiments, but application of ATP only elicited calcium responses in mAL neurons. Furthermore, the *ppk23-LexA* driver (in F+M cells) that we used for M cell activation was sufficient to produce ATP-mediated activation of P1 and PPN1, and these responses were abolished in the presence of Gal80 in F cells. Thus, the observation that M cells activate mAL but not P1 or PPN1 is unlikely due to technical limitations.

This study demonstrates a specific computational logic used by the nervous system to integrate different sensory inputs. Pheromones provide excitatory or inhibitory drives onto P1, such that P1 activity reflects the integration of positive and negative sensory inputs, with female pheromones causing net excitation and male pheromones causing net inhibition. P1 also integrates inputs from other sensory systems, as P1 neurons respond to visual stimuli (Kohatsu and Yamamoto 2015) and olfactory pheromones (Kohatsu, Koganezawa, and Yamamoto 2011; Clowney et al. 2015). Diverse sensory stimuli may alter the weight of excitation versus inhibition onto P1 and bias the decision to court. Taken together, these studies reveal an elegant strategy used by the nervous system in which excitatory and inhibitory inputs directly converge onto a common output to control a significant behavioral decision.

Acknowledgements

Sandra Fendl and Alex Naka assisted with behavioral studies. Cosmos Wang assisted with anatomical studies. The Scott laboratory provided comments on the manuscript.

Methods

Fly strains

The following fly lines were used: *ppk23-LexA* (a gift from Dr. Barry Dickson); *lexAop2-IVS-GCaMP6S-SV40* (Bloomington Drosophila Stock Center [BDSC] #44273)*; ppk25-Gal4* (Starostina et al. 2012); *ppk23-Gal4, lexAop-Gal80, UAS-mCD8::tdTomato (X II III)* (Thistle et al. 2012); *vGlut-Gal4* (*OK371-Gal4*) (Daniels et al. 2008); *vGlut-LexA::VP16* (Baek, Enriquez, and Mann 2013); $vGlut^{MI04979}$*-LexA::QFAD,* $vGlut^{MI04979}$*-QF2* (Diao et al. 2015); *UAS-mCD8::GFP* and *lexAop-CD2::GFP* (Lai and Lee 2006); *UAS-DTI* (Han, Stein, and Stevens 2000); *fru-Gal4* (Stockinger et al. 2005); *fru-LexA* (Mellert et al. 2010); *lexAop2-FLPL(attp40)* (BDSC #55820); *UAS-GCaMP6S* (T.-W. Chen et al. 2013); *UAS-dTRPA1* (Hamada et al. 2008); *UAS-syt-eGFP* (Zhang, Rodesch, and Broadie 2002); *UAS-Denmark* (Nicolai et al. 2010); *UAS-CD4::GFP1-10* and *lexAop-CD4::GFP11* (Gordon and Scott 2009); *UAS-P2X2* (Lima and Miesenböck 2005); *lexAop-P2X2* (Yao et al. 2012) ; *UAS>stop>CD8::GFP,* $UAS>stop>dTRPA1^{myc}$, *UAS>stop>TNTactive, UAS>stop>TNTinactive* (von Philipsborn et al. 2011); *UAS-Empty-RNAi* (BDSC #36303); *UAS-vGAT-shRNA* (BDSC #41958)*; UAS-Dicer2 (X)* (BDSC #24644); *UAS-Dicer2(II)* (BDSC #24650)*; UAS-Rdl-RNAi* (BDSC #31286); *QUAS-Gal80* (BDSC #51950); *P1-Gal4* (Inagaki et al. 2014)*; R71G01-Gal4* (Pan, Meissner, and Baker 2012)*; R43D01-Gal4* (BDSC #48151)*; PPN1-Gal4* (*R56C09-Gal4*, BDSC #39145)*; PPN1-LexA* (*R56C09-LexA*, BDSC #53584)*; UAS-IVS-Chrimson.mVenus(attp18)* (BDSC #55134)*; LexAop2-IVS-Chrimson.mVenus(attp40)* (BDSC #55138)*; UAS-ArcLight* (Cao et al. 2013); *UAS>stop>nsyb-GFP 19a; UAS>stop>Dscam17.1-GFP 19a* (Yu et al. 2010), *QUAS-mCD8::GFP* (BDSC #30003).

Leg bristle G-CaMP imaging

Single bristle imaging was performed as previously described (Thistle et al. 2012). Flies of the genotype *ppk23-LexA*, *LexAop-GCaMP6S, ppk25-Gal4, UAS-CD8::tdTomato* were placed in a custom imaging chamber and their forelegs were secured with wax. Female (7,11-heptacosadiene and 7,11-nonacosadiene) or male (7-tricosene and cis-vaccenyl acetate) pheromone mixes (100 ng/mL, Cayman Chemical) were applied to single bristles on the three distal leg segments for 30 s. G-CaMP responses were captured using a 3i spinning disk confocal system equipped with a 20x air objective and 1.6x optical zoom. Responses in the two PPK23 cells under each bristle were analyzed based on their expression of CD8::tdTomato; M cells were tdTomato-negative, and F cells were tdTomato-positive. The change in fluorescence in each cell was calculated as follows: $100*((F_t-F_0)/F_0)$, where F_0 is the mean fluorescence intensity during the 4 s prior to stimulation.

The heat map in Figure 1B was created in Fiji. The average fluorescence intensity of the 10 frames preceding each stimulation (female and male mixes) was subtracted from the frame at which the fluorescence intensity of the responding cell was at a maximum. The resulting images from each stimulation were then merged into a two-channel image. The channels corresponding to the female or male pheromone stimulation were pseudocolored red and blue, respectively.

Central brain G-CaMP imaging and ATP stimulations

GCaMP imaging experiments were performed as previously described (Harris et al. 2015). Virgin males were collected at eclosion and were aged in isolation for 2 to 6 days before imaging. They were briefly anaesthetized with CO_2 and placed into a small slit on a custom-built

plastic mount at the neck such that the head was isolated from the rest of the body. The head was then immobilized using nail polish. Two small pieces of plastic were affixed with nail polish to the underside of the plastic mount on either side of the thorax, such that the legs were forced into a forward-facing position. The proboscis was covered with wax to prevent labellar taste input. The head cuticle was dissected with fine forceps in ice-cold adult hemolymph-like solution (AHL) (J. W. Wang et al. 2003), and obscuring air sacs and other debris were removed. Eyes were damaged or removed to minimize visual input from the imaging laser. A coverglass was placed at a 45-degree angle to the plane of the plastic mount such that the head was isolated from the rest of the body.

G-CaMP responses were captured using a fixed-stage 3i spinning disk confocal system equipped with a 20x water objective and 1.6x (mAL and P1) or 2.5x (PPN1) optical zoom and a 488 nm laser. During the stimulation, stacks of 15-20 Z-slices (1-1.5 mm/Z-slice, for mAL and P1) or 8-12 Z-slices (0.5-0.8 μm/Z-slice, for PPN1) were obtained with a 100-ms exposure per Z-slice, resulting in each imaging volume/timepoint being acquired every 1.7-3.9 s. For each trial, 20 imaging timepoints were acquired.

For P2X2-mediated stimulation of M and/or F cells, ~4 mL of 100 ATP (adjusted to pH 7) was pipetted onto a small cube of 2% agar, which was placed on the end of a glass capillary (OD 1.0 mm, ID 0.78 mm). The capillary was placed into an electrode holder that was secured to a micromanipulator. The agar cube was advanced such that it touched the flies' legs at timepoint 6 of 20. The cube was left within reach of the flies' legs for 3 timepoints before being removed.

F and M cells were exogenously activated to ensure specific stimulation of different sensory classes. Delivery of synthetic pheromones requires solubilization in ethanol or hexane, solvents that dissolve the fly's endogenous cuticular hydrocarbons, which may independently activate F or M cells. It was possible to apply pheromone solutions to the tip of a single sensory bristle without detriment (Figure 1A).

For PPN1 imaging, because G-CaMP6s baseline fluorescence was very low, a red reporter (*UAS-CD8::tdTomato*) was included in order to visualize axonal endings. One stack of 15-20 Z-slices from the 561 nm laser line was obtained at the beginning of each imaging session. These were later used to define regions of interest for imaging analysis.

Chrimson-mediated activation of PPN1

For PPN1 activation experiments, we fed isolated adult male flies for a minimum of 3 days on standard fly food supplemented with all-*trans* retinal (final concentration 400 mM). These flies, as well as control males fed normal food, were kept in constant darkness until the experiment. Imaging was performed similarly to above ("G-CaMP imaging") except that a 635 nm laser (Laserglow) was directed at the thorax. The laser was turned to its highest power (~0.01 mW/mm^2) but was in standby mode until frame 6 of 20, at which time the key was turned to open the shutter. The laser was left on for 6 frames. During imaging, a 525/45 bandpass emission filter (Semrock) was used to prevent the 635 nm laser light from interfering with the G-CaMP signal. In some cases, we found that the 488 nm imaging laser was sufficient to activate Chrimson and trigger calcium responses in downstream neurons (i.e., ppk23>Chrimson, P1>GCaMP6s). However, this was never observed in PPN1>Chrimson flies, likely due to weak PPN1 or Chrimson transgene expression.

G-CaMP imaging analysis

For Figures 2, 4, and 6D, calcium imaging data were processed in Fiji. For PPN1, a red anatomy scan (with 561 nm laser) measuring CD8::tdTomato fluorescence was taken prior to G-CaMP calcium imaging. A maximum intensity Z-projection for the anatomy scan and each G-CaMP timepoint was used for analysis. The anatomy projection was used to draw an ROI covering the axonal region in the ventrolateral protocerebrum ("anatomical ROI"). A second ROI was drawn in a region lacking both tdTomato and G-CaMP signal ("background ROI"). Mean fluorescence levels from the background ROI was subtracted from the anatomical ROI at each G-CaMP timepoint resulting in the fluorescence trace over time: F_t. DF/F(%) was calculated as follows: $100*((F_t-F_0)/F_0)$, where F_0 is the mean fluorescence intensity during time points 2 to 5. For P1 fibers, DF/F(%) was calculated in the same way, except that in place of an anatomical CD8::tdTomato scan, "anatomical ROIs" covering P1 commisural fibers were drawn using the maximum projection across time of the G-CaMP signal. Maximum DF/F(%) was calculated by subtracting the average DF/F(%) of the 3 timepoints preceding the stimulation from the maximum DF/F(%) of the 4 timepoints following the stimulation. Due to unavoidable differences in the background fluorescence between pre- and post-ablation imaging scans, the DF/F values presented in Fig. 6D were calculated without background subtraction.

For Fig. 5, calcium imaging data were processed in Matlab. ROIs were drawn around mAL cell bodies in single slices. DF/F(%) was calculated as follows: $100*((F_t-F_0)/F_0)$, where F_0 is the mean fluorescence intensity during time points 2 to 5 and F_t is the fluorescence at each timepoint. Maximum DF/F(%) was calculated by subtracting the average DF/F(%) of the 3 timepoints preceding the stimulation from the maximum DF/F(%) of the 4 timepoints following the stimulation.

For the heatmap in Fig. 5A, DF values were calculated for each pixel in each slice at each timepoint, generating a 4-dimensional data set. These data were collapsed spatially into a 3-dimensional data set using a maximum intensity projection in the Z dimension. The heat map represents the maximum DF values that occurred during stimulus (timepoints 6-9). This heatmap was overlaid on a grayscale image that is the maximum intensity projection of the average baseline fluorescence (timepoints 2-5). The color bar scale represents the minimum (blue) to maximum (dark red) DF.

For all G-CaMP data, averaging the DF/F(%) traces across animals required re-sampling the individual DF/F(%) traces at 10 Hz (completed with Matlab using a linear interpolation), due to the variable duration of timepoints between animals.

Two-photon laser-mediated ablations

Ablations were performed on a Zeiss LSM 780 NLO AxioExaminer microscope. Flies expressed G-CaMP6s in both mAL and P1 neurons, visualized using 488 nm light. A rectangular ROI (approximately 5 mm x 15 mm) was drawn to cover the width of the tract carrying mAL axons in a single z-section located in the middle of the tract. We then scanned the ROI 10 times (3.15 ms pixel dwell time) with intense 760 nm light (~50 mW at the front lens). Lesions were considered successful when the mAL axonal tract became discontinous. Mock ablations were performed identically except that the ROI was moved lateral to the mAL axonal tract (at the edge of the optic lobe). All ablations were performed bilaterally. Pre- and post-ablation stimulation of F and M cells were performed on a spinning disk microscope as described above. We waited 10-20 min after the ablation to stimulate the fly with ATP ("post-ablation" condition).

ArcLight imaging with mAL activation

Isolated adult male flies were fed standard fly food supplemented with all-*trans* retinal (final concentration 400 μM) for a minimum of 2 days and were kept in constant darkness until the experiment. Three- to 5-day-old flies were prepared as described above (GCaMP6s imaging). Imaging was performed on a Zeiss LSM 780 NLO AxioExaminer microscope. To find the region of greatest mAL-P1 overlap, Chrimson.mVenus in mAL neurons was briefly imaged with low-intensity 514 nm light, and the ROI to be scanned (approximately 30 μm x 30 μm) was drawn around the distal mAL axons where they interdigitate with P1 fibers ("signal ROI"). A second region of interest ("background ROI") was drawn in an area lacking ArcLight or Chrimson.mVenus fluorescence. ArcLight was excited with 925 nm light and scanned at approximately 15 Hz. To activate mAL neurons, flies were stimulated 5 times (~5 s/stimulation, ~30 s between stimulations) with a 635-nm laser (Laserglow, Canada, ~0.01 mW/mm^2). We observed weak responses in flies expressing Chrimson in mAL but not fed retinal. These responses were significantly smaller than the responses in flies fed retinal.

ArcLight imaging analysis

To calculate F/F of P1 ArcLight signal, the background ROI intensity trace was first subtracted from the signal ROI intensity trace, resulting in F. For each fly, the 5 laser stimulations were then aligned such that laser onset for each stimulation was t = 0 and the average was taken. ΔF/F(%) for each animal was calculated as follows: $100*((F-F_0)/F_0)$, where F_0 is the mean fluorescence intensity over the period from 0.7 to 2.6 s preceding the stimulation. Maximum ΔF/F(%) was calculated by subtracting the average ΔF/F(%) of 2 s preceding the stimulation from the maximum ΔF/F(%) of 2 s following the stimulation.

Courtship behavior

Courtship behavior experiments were performed essentially as described (Thistle et al. 2012), with the following modifications: male-female assays were recorded for 10 min; assays involving *UAS-dTRPA1* were performed at room temperature (~23°C) and 30°C; for Fig. 3e, due to the relative weakness of *UAS>stop>TRPA1*^{myc}, male flies were pre-incubated at 30°C for 5 min before being presented with a female; assays involving Chrimson were performed under white light (~0.05 mW/mm^2) with male flies fed 400 mM all-*trans* retinal for a minimum of 3 days in the dark. We found that bright white light was sufficient to activate Chrimson and cause behavioral phenotypes.

Immunohistochemistry

Antibody staining and immunohistochemistry were performed as previously described (Z. Wang et al. 2004). The following primary antibodies were used: rabbit anti-GFP (Invitrogen, 1:1,000), mouse anti-GFP (Invitrogen, 1:1,000), mouse anti-nc82 (Hybridoma Bank, 1:500), rabbit anti-RFP (Clontech, 1:500); rabbit anti-GABA (Sigma, 1:1,000); rabbit anti-FruM (1:100). For GRASP experiments, we used a mouse monoclonal antibody that specifically recognizes reconstituted GFP (Sigma, 1:200). Secondary antibodies were Alexa Fluor goat anti-mouse 488, goat anti-rabbit 488, goat anti-mouse 568, goat anti-rabbit 568 (Life Technologies, 1:100).

Transgene generation

To generate *R43D01-LexA*, a 1157-bp fragment from genomic DNA, including the entire R43D01 tile from the FlyLight collection (Pfeiffer, Truman, and Rubin 2012), was amplified using the primers ttgagcacggatttcagcag and ggggtcctcaaatgtgtcgatttgt. This fragment was

recombined into the pBPLexA::p65Uw plasmid (Pfeiffer et al. 2010), and inserted into the VK00018 landing site (Venken et al. 2006).

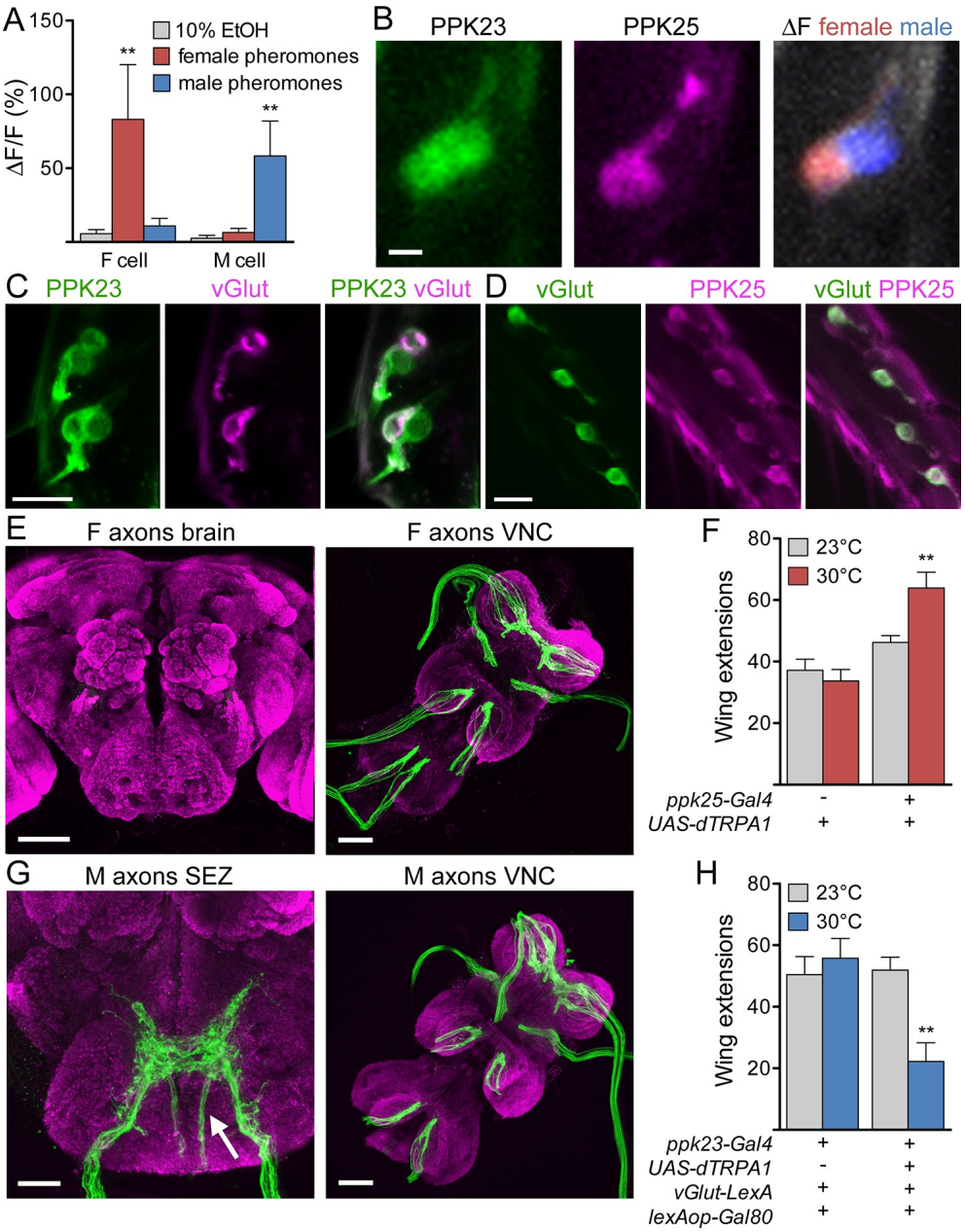


Figure 2.1: F and M cells comprise distinct chemosensory neuron classes.

A. F cells (PPK23+ PPK25+) respond to female pheromones whereas M cells (PPK23+ PPK25-) respond to male pheromones; n = 7 bristles. The female pheromone mix contained 7,11-heptacosadiene and 7,11-nonacosadiene. The male pheromone mix contained 7-tricosene and cis-vaccenyl acetate.

B. GCaMP6s marks two PPK23 cells per bristle (left). CD8::tdTomato marks the PPK25 cell (middle). Maximum ΔF of both PPK23 cells to female (red) or male pheromones (blue) (right).

C. vGlut (magenta) is expressed in one PPK23 cell (green) under each bristle. Transgenic flies with *ppk23-LexA, lexAop-CD2::GFP, vGlut-Gal4, UAS-CD8::tdTomato* were used for cell labeling.

D. vGlut (green) and PPK25 (magenta) are expressed in the same cell under each bristle. Flies contained *vGlut-LexA::VP16, lexAop-CD8::GFP, ppk25-Gal4, UAS-CD8::tdTomato*.

E. Axons from F cells in the legs (green) do not project to the central brain (left) but instead terminate in the six leg neuromeres of the ventral nerve cord (VNC, right). Brains are counterstained with nc82 (magenta) to show neuropil.
F. Expression of dTRPA1 in F cells promoted male-female courtship upon heat-evoked neural activation; n = 11-21/condition. Number of unilateral wing extensions per 10-minute trial was recorded.
G. M cells from the legs project to the SEZ in the brain (arrow shows fibers entering from the cervical connective) and VNC. Other SEZ axons come from the proboscis, with fibers entering from the labellar nerve.
H. dTRPA1-mediated activation of M cells suppressed male-female courtship. n = 10-12/condition. Number of unilateral wing extensions per 10-minute trial was recorded.
Scale bars, 5 (B), 10, (C, D) 25 (G, SEZ) or 50 μm (E, G, VNC). Data are Mean ± SEM. Kruskal-Wallis test, Dunn's post-hoc (A) or 2-way ANOVA, Bonferroni post-hoc (F, H). $^{**}p < 0.01$. See also Figure S1, on selectively targeting F or M cells.

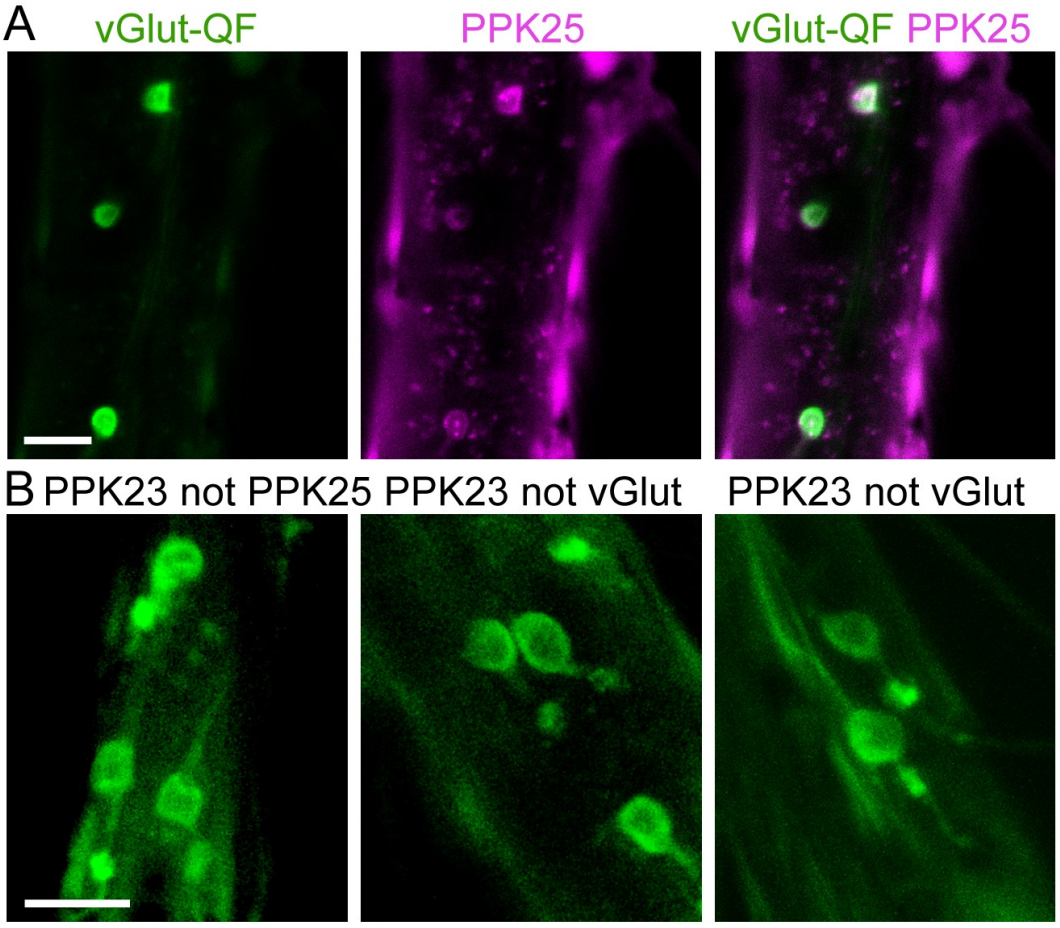


Figure 2.2: A genetic approach to selectively target F or M cells.
A. *vGlut-QF* (green) is expressed in PPK25 cells (magenta), similar to *vGlut-LexA* in Figure 2.1D. Flies were *vGlut-QF2, QUAS-Gal80, ppk25-Gal4, UAS-CD8::tdTomato*.
B. (left), Ablating F cells (*ppk25-Gal4*) using diphtheria toxin leaves M cells intact. This strategy was used to label M cells in Fig. 1G. (middle), Suppressing Gal4-dependent expression in F cells (*ppk23-Gal4, UAS-CD8::tdTomato, vGlut-LexA*, *lexAop-Gal80*) leaves expression intact in M cells. This strategy was used to activate M cells in Fig. 1H. (right), Suppressing LexA-dependent expression in F cells (*ppk23-LexA, lexAop-CD2::GFP, vGlut-QF2*, *QUAS-Gal80*) leaves expression intact in M cells. This strategy was used to activate M cells in Figs. 2B, 4B, and 5E. Different approaches were used to accommodate chromosome locations of transgenes. Scale bars, 10 μm.

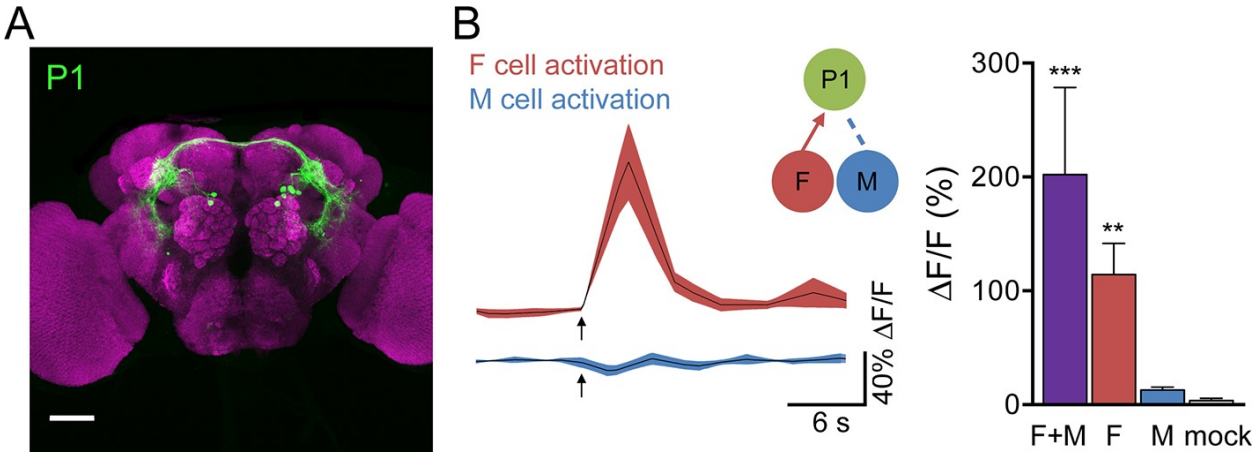


Figure 2.3: F cells activate courtship-promoting P1 neurons.
A. Male-specific P1 neurons (green) are located in the protocerebrum. Scale bar, 50 μm. Flies contained *P1-Gal4DBD*, *P1-Gal4AD, UAS-CD8::GFP*.
B. ATP-mediated stimulation of F+M cells (*ppk23-LexA, lexAop-P2X2*), F cells (*vGlut-LexA*) but not M cells (*ppk23-LexA, lexAop-P2X2, vGlut-QF2, QUAS-Gal80*) triggered calcium increases in P1 neurons; n = 5–8/condition. Mock is no P2X2. Traces on the left show averaged ΔF/F with mean in black and SEM shaded. Arrows indicate stimulus. Schematics show cells monitored with GCaMP6s (green) and connections tested. Data are also displayed as bar graph (right). Differences in expression levels of *ppk23-LexA* and *vGlut-LexA* may contribute to different response magnitudes of F+M versus F cell stimulation. Mean ± SEM of maximum ΔF/F. Kruskal-Wallis test, Dunn's post-hoc to mock, *p<0.05, **p<0.01, ***p<0.001.

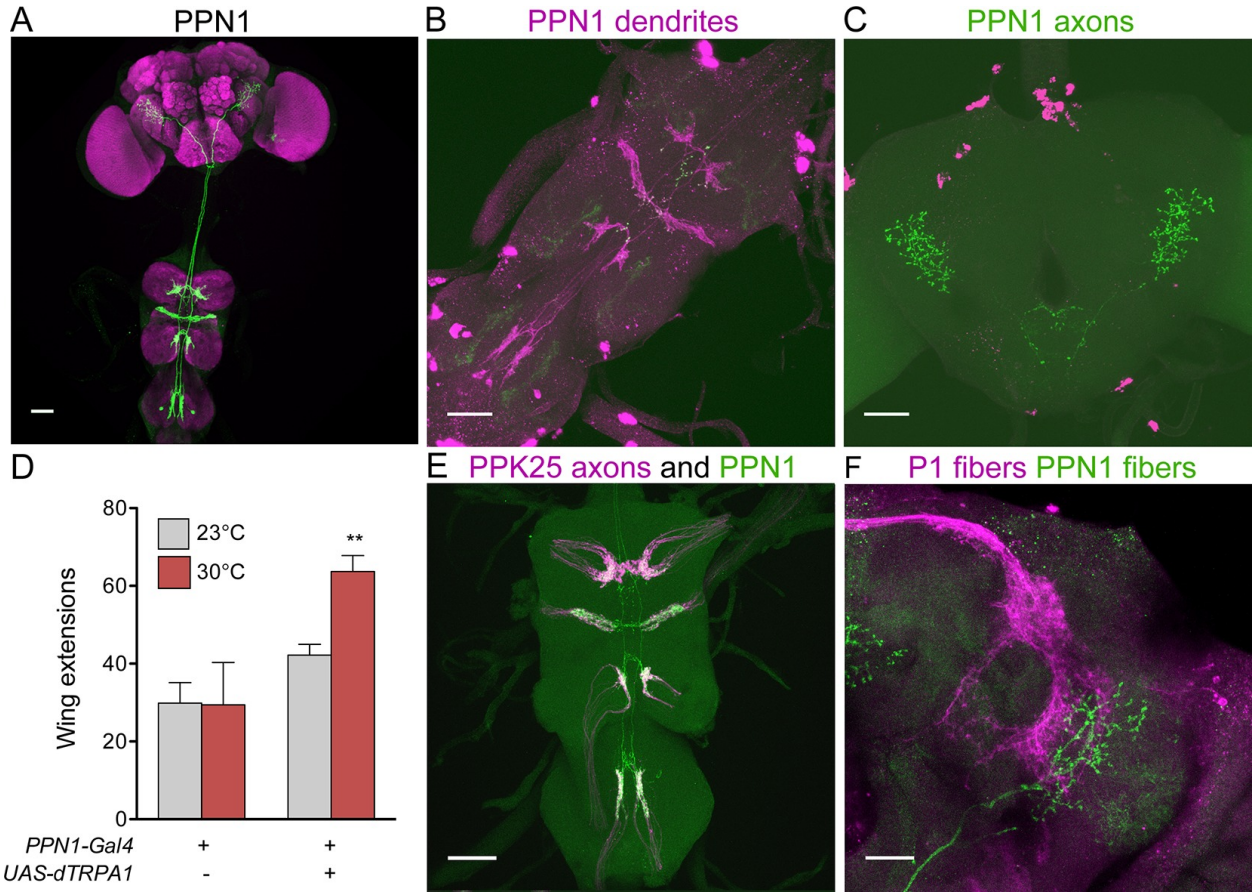


Figure 2.4: PPN1 neurons are courtship-promoting neurons in proximity to PPK23 axons and P1 fibers

A. PPN1 neurons have cell bodies in the third leg neuromere of the VNC and send projections to the six leg neuromeres and wing neuromere of the VNC and to the ventrolateral protocerebrum of the brain. *R56C09-Gal4* drives expression of *UAS-CD8::GFP* exclusively in the pair of PPN1 neurons.

B-C. PPN1 has dendrites in the VNC (B, DenMark, magenta) and axons in the ventrolateral protocerebrum (C, syt-GFP, green). B and C are from the same animal containing *R56C09-Gal4, UAS-DenMark, UAS-synaptotagmin-GFP*.

D. Activation of PPN1 with dTRPA1 causes increased male-female courtship at 30°C; mean ± SEM, n = 16-30/condition, $^{**}p < 0.01$ (2-way ANOVA, Bonferroni post-hoc).

E. Overlap is observed in the VNC between PPN1 dendrites (magenta) and incoming PPK23 axons (green). *R56C09-Gal4, UAS-CD8::tdTomato, ppk23-LexA, lexAop-CD2::GFP* flies were used.

F. Overlap between PPN1 (green) and P1 (magenta) in the anterior ventrolateral protocerebrum (50 µm collapsed Z-stack). Scale bars, 25 µm (F) 50 µm (A-E).

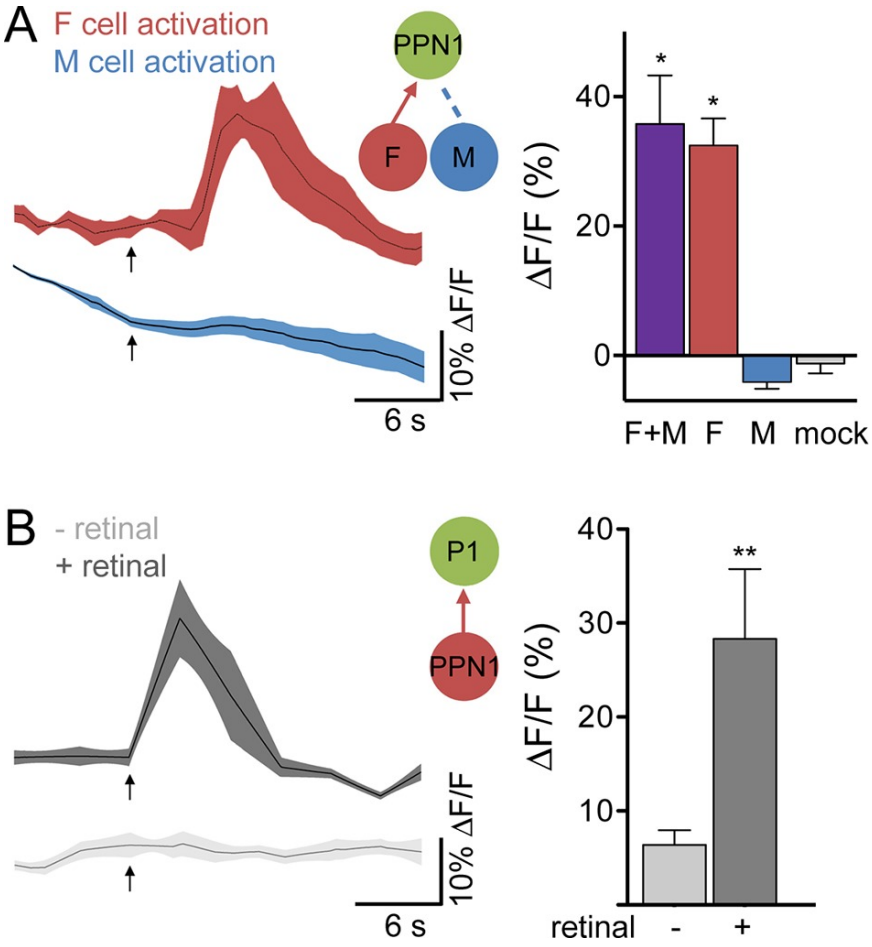


Figure 2.5: F cells activate courtship-promoting PPN1 neurons which activate P1.
A. Calcium imaging of PPN1 axons while activating different sensory classes revealed that PPN1 is activated by F+M and F cell stimulation but not M cell stimulation; n = 5–7/condition. Mock is no P2X2. Arrows indicate stimulus.
B. Chrimson-mediated activation of PPN1 triggers calcium increases in P1 by GCaMP6s calcium imaging; n = 5–6/condition. Arrows indicate stimulus. Schematics show cells monitored with GCaMP6s (green) and connections tested. Data are Mean ± SEM. Kruskal-Wallis test, Dunn's post-hoc to mock (A) or Mann-Whitney test (B). *p<0.05, **p<0.01.

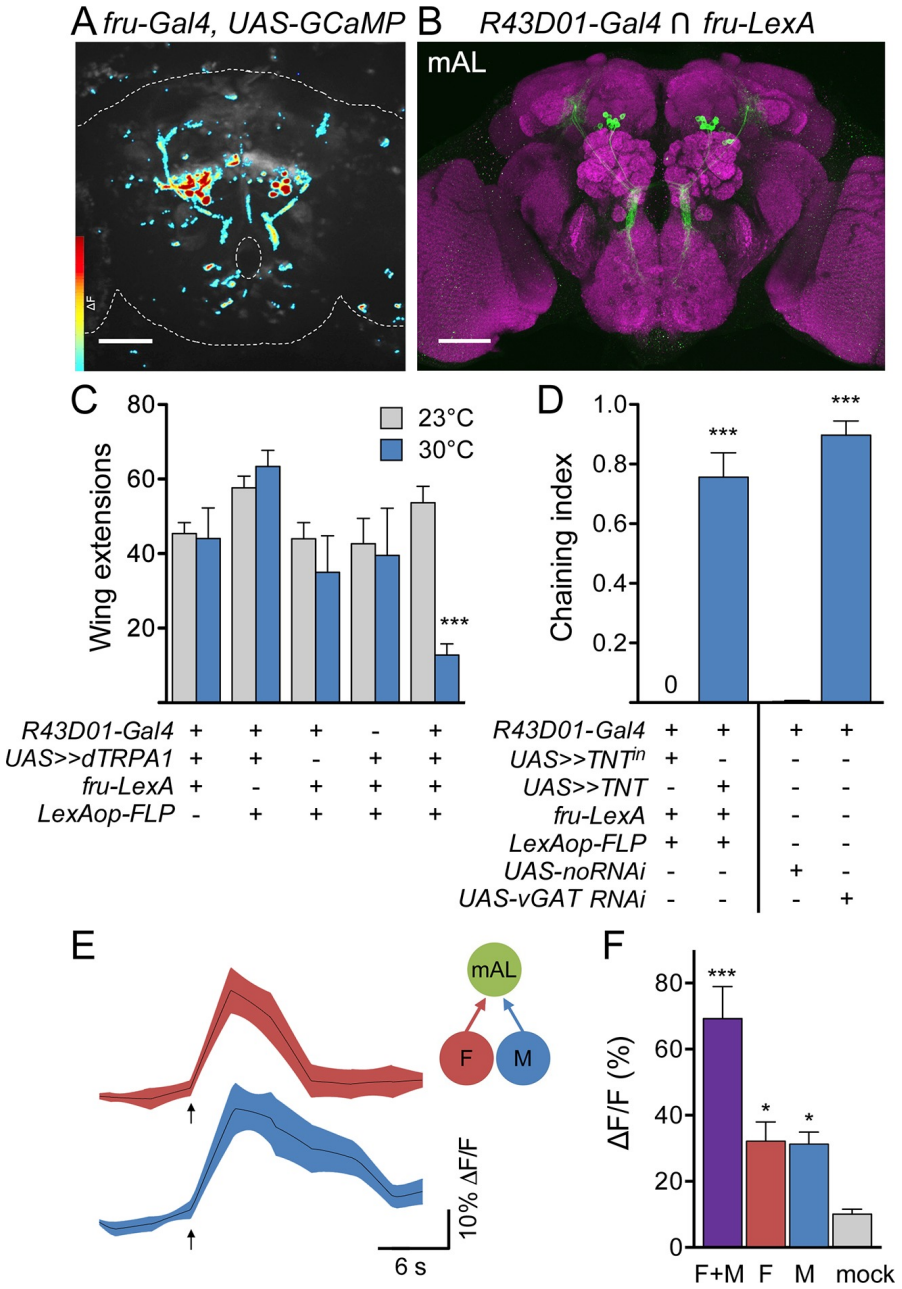


Figure 2.6: M cells and F cells activate courtship-suppressing mAL neurons.

A. Example image of a GCaMP6s ΔF heat map in *fru-LexA* neurons upon P2X2-mediated activation of M cells.

B. mAL neurons labeled by the intersection of *R43D01-Gal4* and *fru-LexA* connect the SEZ and protocerebrum.

C. Activating mAL neurons with dTRPA1 suppresses courtship toward females; n = 10/condition.

D. Silencing mAL neurons with tetanus toxin or knocking down vGAT with *R43D01-Gal4* induces male-male chaining; n = 8-10 groups/condition, 6-9 males per group. For C and D, >> means >stop>. Chaining index represents the fraction of time 3 or more males were courting over the 10-min trial.

E. P2X2-mediated stimulation of either F or M cells activates mAL neurons by GCaMP calcium imaging. Arrows indicate stimulus.
F. Maximum ΔF/F in mAL cell bodies; n = 5-9/condition. Mock is no P2X2.
Scale bars, 50 μm (A, B). Data are Mean ± SEM, 2-way ANOVA, Bonferroni post-hoc (C), Mann-Whitney test (D), or Kruskal-Wallis test, Dunn's post-hoc to mock (F). $^{*}p < 0.05$, $^{***}p < 0.001$.

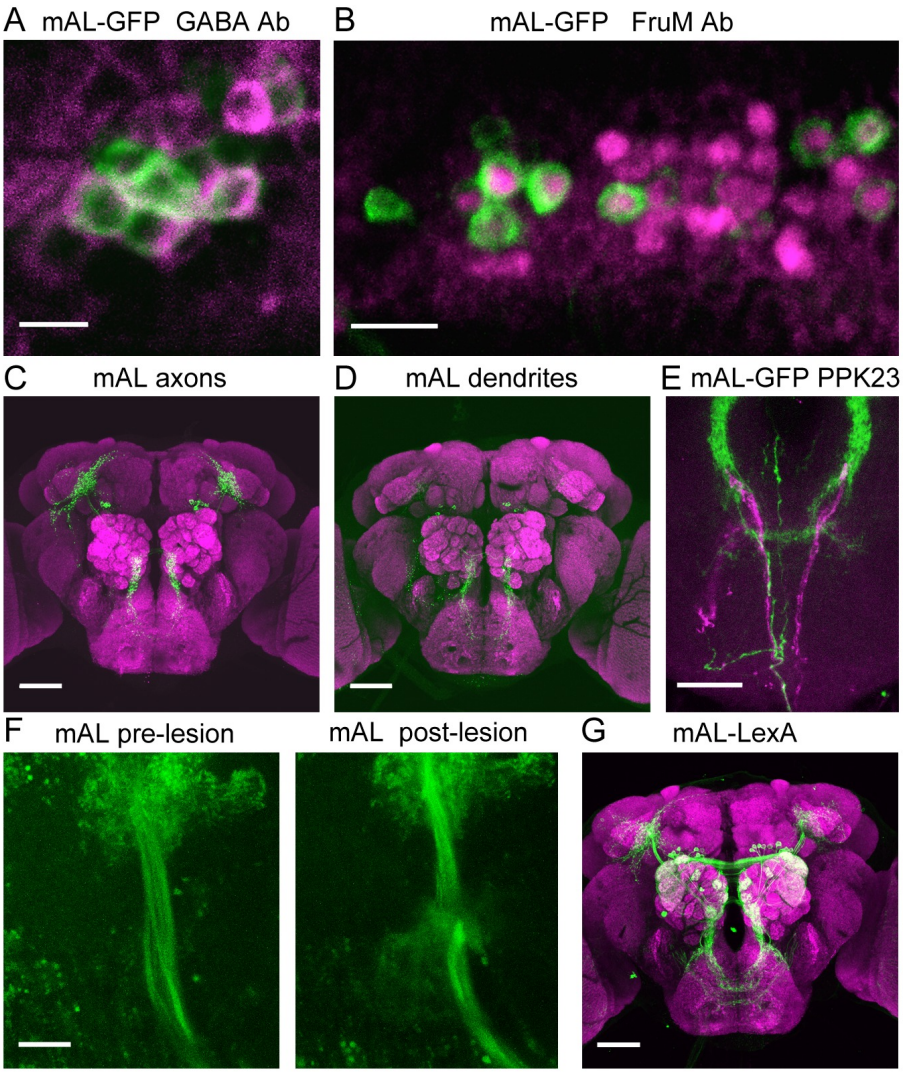


Figure 2.7. mAL neurons are GABAergic neurons that connect the SEZ and higher brain.
A. mAL neurons labeled by *R43D01-Gal4* (green, CD8::GFP) are immunopositive for GABA (magenta).
B. mAL neurons labeled by *R43D01-Gal4* (green, CD8::GFP) express Fru^{M} (magenta).
C. mAL neurons have presynaptic termini (green, nsyb-GFP) in the higher brain and SEZ.
D. mAL neurons have dendrites (green, Dscam17.1-GFP) primarily in the SEZ.
E. M cell axons (magenta, myr::mCherry) interdigitate with mAL fibers (green, CD8::GFP) in the SEZ.
F. A representative image of the mAL axonal tract in the higher brain before and after 2-photon-mediated lesioning.
G. *R43D01-LexA* labels mAL neurons and some olfactory sensory neurons (green, CD2::GFP).
Scale bars, 5 μm (A), 10 μm (B, F), 25 μm (E), 50 μm (C, D, G).

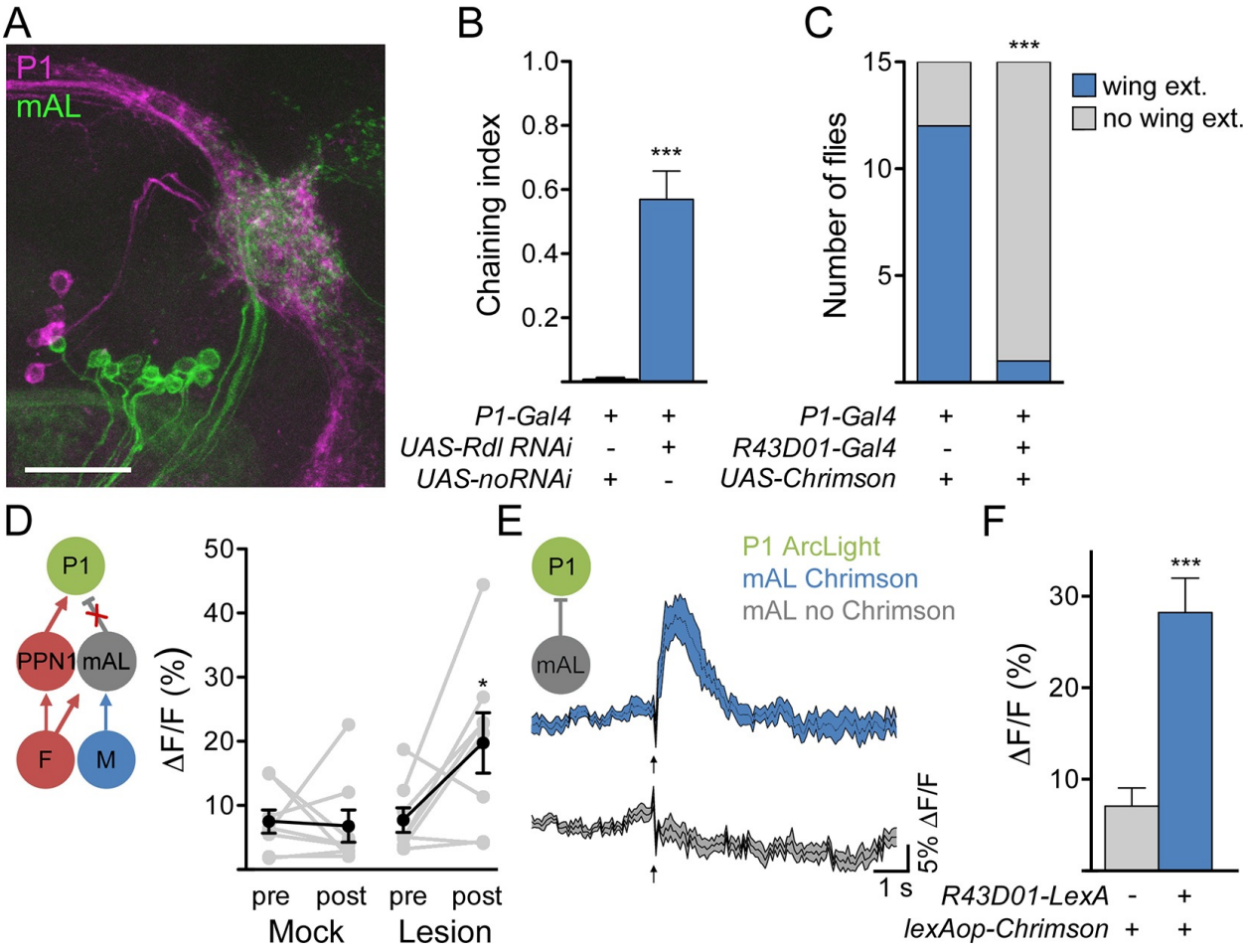


Figure 2.8: mAL neurons functionally and behaviorally inhibit P1 neurons.
A. Overlap between mAL (green) and P1 (magenta) (collapsed 97-µm stack). Scale bar is 25 µm.
B. Knockdown of $GABA_A$ receptor Rdl in P1 neurons induces male-male chaining, n = 10/condition.
C. Chrimson-mediated activation of P1 neurons causes wing extension (wing ext.) in solitary males, which is suppressed by co-activation of neurons expressing *R43D01-Gal4*.
D. Lesioning mAL axons increases G-CaMP response in P1 upon P2X2-mediated stimulation of F+M cells.
E. Chrimson-mediated activation of mAL neurons causes P1 hyperpolarization, as detected by increased ArcLight fluorescence. Arrow indicates laser.
F. Maximum ΔF/Fin P1; n = 10–11/condition. Mann-Whitney test (B, F), Fisher's exact test (C), or paired t-test (D). $^{*}p < 0.05$, $^{**}p < 0.01$, $^{***}p < 0.001$.

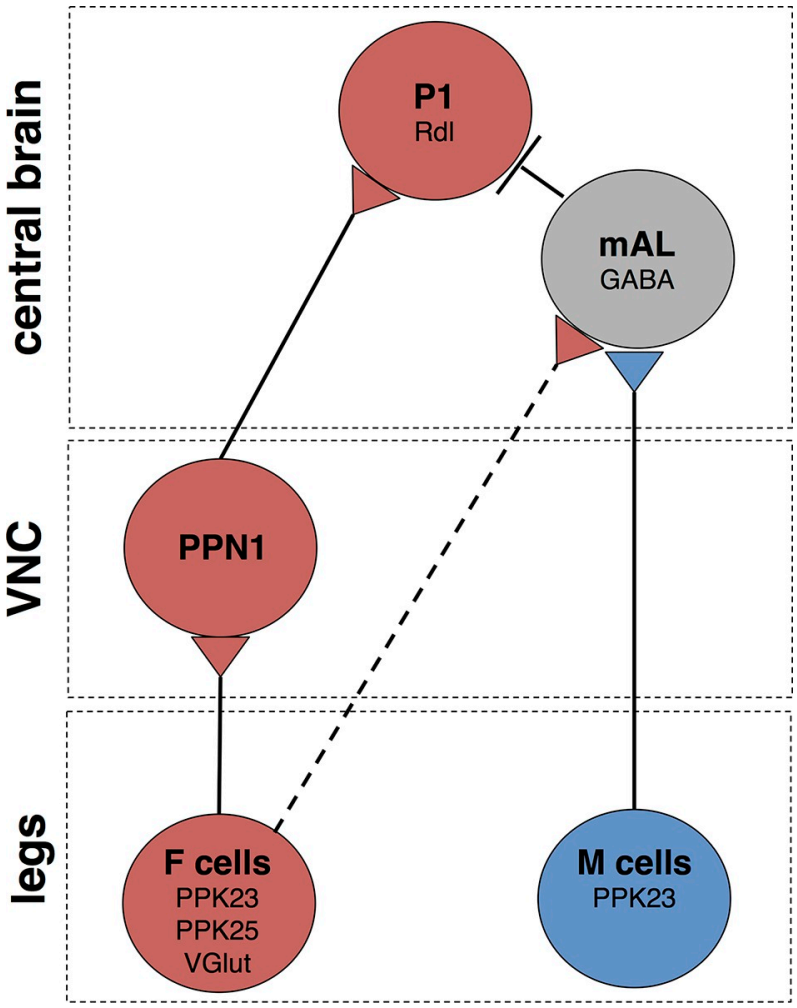


Figure 2.9. Schematic of courtship-promoting and courtship-inhibiting circuits activated by F and M cells.

F cells on the leg express PPK23, PPK25, and VGlut, and respond to female pheromones. M cells on the leg express PPK23 and respond to male pheromones. The M cell neurotransmitter is unknown. F cells activate PPN1, a class of projection neuron with cell bodies and dendrites in the VNC and long-range axonal projections to the ventrolateral protocerebrum. PPN1 axons are in close proximity to P1 fibers, and PPN1 activation causes activation of P1. M cells on the leg activate GABAergic mAL neurons, which connect the SEZ and superior lateral protocerebrum. mAL axons interdigitate with P1 fibers, and mAL activation causes hyperpolarization of P1, likely through the GABA-A receptors containing the Rdl subunit. F cells also provide an inhibitory drive onto P1 via mAL. The contact between F cells and mAL is not direct (dotted line). Other connections may not be monosynaptic.

CHAPTER 3

Optical methods to label taste-responsive neurons

Summary

Studies identifying gustatory receptors and the sensory cells in which they are expressed have demonstrated that taste cell responses are modality-specific. The logic of how taste information is processed by central circuits is unknown. Using large-scale calcium imaging in conjunction with cell labeling, we show that sweet and bitter sensory cells activate largely non-overlapping populations of neurons throughout the subesophageal zone (SEZ) and that circuits for sweet and bitter tastes are segregated from sensory input to motor output. We used an optimized version of this experimental strategy to begin to identify neuronal components of SEZ taste circuits. Unexpectedly, we gather evidence suggesting that a class of second-order olfactory neurons may also be activated by aversive bitter stimuli.

Portions of this work have been previously published as:

Harris D.T., Kallman B.R., Mullaney B.C., Scott K. Representations of taste modality in the *Drosophila* brain. *Neuron* 86 (6): 1449–60

Introduction

The gustatory system allows animals to distinguish between nutritious and noxious substances in their environments and thus is crucial to their survival. The sensory receptors that detect these substances, as well as the peripheral sensory neurons in which they are expressed, have been identified in mammals and invertebrates, but little is known about how taste information is processed by neural circuits in the brain. The fruit fly *Drosophila melanogaster* provides an attractive model system to investigate these questions, as it comes with an extensive genetic toolbox with which to interrogate the functional and behavioral roles of specific neurons or neuronal classes.

Drosophila sense taste compounds with gustatory receptor neurons (GRNs) located on their proboscis, wings, and legs (Stocker 1994). Each GRN is tuned to a different taste modality based on the set of sensory receptors it expresses. In general, each GRN detects one of four taste modalities: sweet, bitter, water, or pheromone. GRNs located on the proboscis send axons into a region of the central brain called the subesophageal zone (SEZ), while leg GRNs send axons to the ventral nerve cord (VNC), analogous to the mammalian spinal cord. Some leg GRNs also send axons directly the SEZ. The axons of differently tuned GRNs are anatomically segregated in the SEZ and VNC. For example, bitter-sensing GRN axons form a ring-like structure in the SEZ, while sweet-sensing GRN axons project lateral to this ring in a non-overlapping manner (Z. Wang et al. 2004).

As taste-responsive circuits in the central brain are largely unknown, the anatomical identification of taste-responsive neurons is an important first step towards understanding the neural circuits underlying taste detection and taste-guided behavior. Only a few classes of taste-responsive neurons have so far been characterized. Previous studies have limited their investigations to random populations of neurons labeled by sparsely expressing Gal4 lines. These studies relied on targeted expression of different versions of the genetically encoded calcium indicator G-CaMP to neurons of interest, allowing for the monitoring of calcium responses in response to different tastants. Two studies identified three different classes of proboscis motor neurons and showed that these neurons respond most strongly to sugar and water, both palatable stimuli, while responding weakly or not at all to caffeine, a bitter compound (Gordon and Scott 2009; Manzo et al. 2012). More recent studies have identified two classes of sugar-responsive SEZ interneurons, both of which also exhibit modality-specific taste responses (Flood et al. 2013; Yapici et al. 2016).

Thus, while the handful of taste-responsive neurons so far identified appear modality-specific, whether this paradigm is true for all taste-responsive neurons has remained unclear. The major drawback of previous Gal4-based approaches is the limited number of neurons whose activity can be monitored simultaneously. The advent of large-scale calcium imaging with improved calcium indicators provides a more unbiased and comprehensive way to identify taste-responsive neurons. Coupled with cell-labeling techniques, this approach could also theoretically permit the anatomical visualization of any taste-responsive neuron in the fly brain.

We employ this strategy to ask how tastes are represented in the SEZ. We show that sugar, bitter, and water tastes activate different populations of neurons throughout the SEZ, with the vast majority of cells responding to a single taste modality. Using a photoactivatable GFP (PA-GFP) to label the entire complement of proboscis motor neurons, we demonstrate that pathways for sweet and bitter tastes are segregated from sensory input to motor output. Nonetheless, we were unable to reliably label individual taste-responsive neurons in the SEZ

using this strategy. This was likely due to the high background fluorescence of pan-neuronally expressed G-CaMP6S in the neuropil, making it extremely difficult to visualize a single PA-GFP-filled fiber.

In order to increase the signal to noise of photoconverted PA-GFP within dense neuropil, we modified our imaging approach to include a pan-neuronal nuclear-localized G-CaMP. This greatly reduced background fluorescence and allowed us to reliably fill a cluster of bitter-responsive neurons in the SEZ. Surprisingly, the anatomical location and distinct morphology of these cells suggested that they were in fact a class of inhibitory olfactory projection neurons (iPNs). This was confirmed by calcium imaging of neurons labeled by an iPN-specific Gal4 line in response to bitter cell activation as well as natural bitter tastants. Thus, at least a subset of iPNs appear to be multimodal inhibitory neurons whose activity may affect the processing of both olfactory and gustatory stimuli. Identification of iPNs as taste-responsive neurons demonstrates the power of our strategy, but whether it will be effective in identifying other components of taste circuits is an open question and may require further troubleshooting.

Results

Large-scale calcium imaging permits identification of taste circuits from input to output

To ask how tastes are represented in the SEZ, the first taste relay in the fly brain, we used a large-scale calcium imaging approach. We generated flies that expressed the genetically encoded calcium indicator G-CaMP6S under control of the pan-neuronal *nSynaptobrevin-Gal4* driver, allowing us to monitor taste responses in all neurons in an unbiased manner. We included a ubiquitously expressed histone-RFP to unambiguously identify the G-CaMP fluorescence changes of single neurons. We then used spinning disk confocal microscopy to image G-CaMP responses while stimulating the proboscis with different tastants. By applying tastants of different modalities, we were able for the first time to create a map of taste quality representation in the SEZ. We found that the vast majority of SEZ neurons respond to either sugar or bitter, but not both (Figure 3.1A-D), arguing that tastes are processed along a labeled line.

We next asked whether this large-scale calcium imaging technique could report the activity of entire sensorimotor circuits from sensory input to motor output. To this end, we asked whether proboscis motor neurons (MNs) were among the responding cells, as subsets of MNs have been shown to respond to sucrose and elicit proboscis extension (Gordon and Scott 2009; Manzo et al. 2012). To identify proboscis MNs and determine their taste responses, we undertook a "back-filling" strategy using photoactivatable GFP (PA-GFP). At baseline, PA-GFP fluoresces weakly, but its fluorescence increases greatly after photoconversion with 800-nm two-photon targeting (Datta et al. 2008; Ruta et al. 2010). We generated flies co-expressing pan-neuronal G-CaMP6S and two copies of PA-GFP, and we stimulated the proboscis with sucrose while monitoring activity in the SEZ using spinning disk microscopy. After the tastant stimulation, we acquired a pre-photoactivation Z-stack of the entire SEZ. We then used a Phasor spatial light modulator coupled to a femtosecond laser to repeatedly scan the pharyngeal and labellar nerves—which carry MN axons—with 800-nm light to photoconvert GFP. A post-photoactivation Z-stack was acquired, and the pre-photoactivation Z-stack was subtracted to yield an image of back-filled neurons. Using this approach, we reliably back-filled the majority of MNs (19 ± 1 cells, compared to a total of 30 MNs reported in previous anatomical studies) (Rajashekhar and Singh 1994). By overlaying the image of back-filled neurons on a ΔF image of the G-CaMP response to sucrose, we were also able to demonstrate that approximately two-thirds (12 ± 1) of the back-filled MNs were sucrose-responsive (Figure 3.2A-D). The other one-third of the MNs may respond to bitter substances and promote proboscis retraction.

An improved strategy to visualize taste-responsive neurons

A previous study that employed the GFP reconstitution across synaptic partners (GRASP) technique demonstrated that taste sensory neurons do not directly contact motor neurons, arguing that one or more interneurons relay taste sensory activation to drive motor programs (Gordon and Scott 2009). Neither the identity nor the number of these interneurons is known. The MN studies suggest that large-scale calcium imaging coupled to cell labeling is a feasible strategy to identify components of taste circuits. Thus, we attempted to use this approach to label non-motor taste-responsive SEZ neurons. Again, we stimulated the proboscis with sucrose or bitter compounds to identify responding neurons, and then used two-photon targeting to photoconvert PA-GFP in individual neurons. While we were able to achieve high levels of PA-GFP photoactivation in the somata of taste-responsive neurons and could often observe proximal portions of a projecting neurite, in general it was difficult to visualize the complete

morphology of a single neuron, especially its relatively small dendritic arbors and axonal termini (Figure 3.3A). In some cases, it was possible to visualize most or all of a given neuron, but these cases were limited to neurons with large cell bodies, which are primarily MNs (Figure 3.3B).

We hypothesized that our inability to trace filled neurons was due to the high baseline fluorescence of cytosolic G-CaMP6S in the neuropil. In order to increase the signal-to-noise ratio of filled cells, we generated flies that expressed a nuclear-localized G-CaMP6S and PA-GFP under control of the pan-neuronal *nSynaptobrevin-Gal4* driver. This greatly lowered the baseline fluorescence of the SEZ neuropil (data not shown). In order to activate sensory neurons in a more high-throughput and reliable manner, these flies also expressed the red-shifted channelrhodopsin CsChrimson under control of the *Gr5a-LexA* or *Gr66a-LexA* drivers, which are expressed specifically in sugar- or bitter-sensing neurons, respectively. We used two-photon calcium imaging to monitor the fluorescence of subsets of SEZ neurons while activating sensory neurons with short pulses of red light from a 635-nm laser. Individual neurons exhibited large, reliable red-light-triggered calcium responses (Figure 3.4A), indicating that nuclear-localized GCaMP6S reports stimulus-driven calcium responses. On the same two-photon microscope, we then targeted responding neurons for photolabeling by drawing a small region of interest (ROI) around the responding nucleus and scanning it repeatedly with photoconverting 780-nm light.

A class of olfactory projection neurons responds to activation of bitter cells

When we activated CsChrimson-expressing bitter sensory neurons with red light, we reliably detected responses in a small number of dorsally located SEZ neurons with cell bodies immediately ventral to the antennal lobe (AL) (Figure 3.4A). We then targeted these cells for photoconversion. Because of movement inherent to the *in vivo* preparation, we were unable to fill individual responding neurons, and instead typically filled a small cluster of approximately 5-7 neighboring cells. Nonetheless, we observed that all of the filled neurons had similar morphology and generally targeted the same regions, suggesting they comprise a distinct neuronal class. They arborized in multiple AL glomeruli and appeared to connect the AL to the lateral horn (LH) through a distinct antennocerebral tract (Figure 3.4B). Through a review of different AL-innervating cell types, we concluded that the filled neurons resembled a previously characterized class of inhibitory olfactory projection neurons (iPNs). In contrast to excitatory projection neurons (ePNs), which typically innervate a single olfactory glomerulus, iPNs are multiglomerular and send axons to the LH via the mediolateral antennal lobe tract (mlALT), bypassing the mushroom body calyx (Tanaka, Endo, and Ito 2012).

To confirm that the bitter-responsive neurons that we filled were indeed iPNs, we imaged the calcium responses of the approximately 45 iPNs that are labeled by the *Mz699-Gal4* driver (Parnas et al. 2013; Liang et al. 2013; Strutz et al. 2014). While *Mz699-Gal4* labels other neurons—including putative third-order olfactory neurons in the ventrolateral protocerebrum (vlpr)—the stereotypical location of iPN cell bodies allowed us to confidently target them for calcium imaging. Individual iPNs exhibited reliable red-light-triggered calcium responses (Figure 3.4C), arguing that a subpopulation of iPNs is activated by bitter stimuli. As further confirmation, we also imaged iPN responses to natural bitter compounds. Applying a mix of 100 mM caffeine and 10 mM denatonium to the proboscis elicited calcium responses in iPN cell bodies, dendrites, and axons (Figure 3.4D). These data argue that a class of olfactory second-order neurons also receives aversive gustatory input.

Conclusions

By employing large-scale calcium imaging in conjunction with cell labeling, we show that taste is processed along a labeled line in the *Drosophila* brain and that responses to tastes in the SEZ, the primary taste relay, are largely modality-specific. We demonstrate that this segregation is maintained in the response profiles of proboscis motor neurons, suggesting that different tastes are processed by different neurons from sensory input to motor output. This paradigm appears to be conserved, as neurons in the primary gustatory cortex of mice are also tuned to a single taste modality and are anatomically segregated into non-overlapping "hot spots" (X. Chen et al. 2011). Labeled-line processing may thus be an evolutionarily effective strategy to interpret taste stimuli and produce robust behaviors.

While it was possible to reliably back-fill motor neurons by targeting the nerves innervating the SEZ, visualizing the morphology of single SEZ neurons proved difficult. Although the somata of targeted cells generally increased greatly in fluorescence after photoactivation, it was challenging to trace their small, weakly labeled fibers more than a few microns. We hypothesized that this was due to the high baseline fluorescence of pan-neuronally expressed cytosolic G-CaMP6S in the neuropil, limiting our ability to resolve the spectrally overlapping PA-GFP within single fibers. We sought to overcome this problem by using a nuclear-localized G-CaMP6S, which we correctly predicted would lessen baseline neuropil fluorescence. Importantly, we could detect large, reliable calcium responses with nuclear G-CaMP6S. Using this improved strategy, we were able to reliably fill a cluster of SEZ neurons that responded to CsChrimson-mediated activation of bitter sensory neurons. These neurons—which arborized in the antennal lobe and sent axonal projections through a distinct tract to the lateral horn—bore a marked resemblance to a class of inhibitory GABAergic olfactory projection neurons termed iPNs. We confirmed that iPNs respond to CsChrimson-mediated activation of bitter cells by imaging G-CaMP6S responses of neurons labeled by *Mz699-Gal4*, an iPN-specific driver line. We also demonstrated that iPNs respond to stimulation of the proboscis with natural bitter tastants.

The finding that iPNs may be multimodal is interesting and unexpected. Several recent studies have examined the role of iPNs in olfactory processing. By monitoring the odor responses of third-order ventrolateral protocerebrum (vlpr) neurons before and after lesioning iPN input to the LH, it was shown that iPNs normally inhibit vlpr neuron responses to food odors but, interestingly, not pheromones (Liang et al. 2013). A concurrent study showed that silencing iPNs weakens flies' ability to discriminate two closely related odors and argued that iPNs normally impose a high-pass filter on inputs from canonical excitatory PNs, blocking weak inputs to third-order vlpr neurons and thus enhancing discrimination (Parnas et al. 2013).

The fact that a subset of iPNs responds to both CsChrimson-mediated activation of bitter cells and natural bitter tastants suggests two non-mutually exclusive models. First, aversive taste may influence the processing of odors through iPNs. It will be interesting to test whether co-presentation of bitter tastants or simultaneous CsChrimson-mediated activation of bitter-sensing cells inhibits the food odor responses of excitatory PNs or third-order vlpr neurons. Second, iPNs may be components of circuits controlling proboscis extension or feeding. The LH is known to be a center for innate behavior, suggesting that iPN input to this region may control descending pathways that then directly influence premotor or motor activity in the SEZ. Testing the effect of activating or silencing iPNs on proboscis extension or food consumption will clarify whether this model is plausible.

Methods

Fly strains

The following fly lines were used: *Gr66a-LexA*, *Gr5a-LexA* (Gordon and Scott 2009), *LexAop2-IVS-Chrimson.mVenus(attp18)* (Bloomington Drosophila Stock Center #55137), *nSyb-Gal4* (Pauli et al. 2008), *UAS-GCaMP6S* (T.-W. Chen et al. 2013), *UAS-NLS-GCaMP6S* (a gift from Dr. Barry Dickson), *UAS-C3PA-GFP* (Ruta et al. 2010), *Mz699-Gal4* (Lai et al. 2008).

Spinning disk calcium imaging with tastant stimulations

Female flies (2–3 days old) were food deprived on a wet Kimwipe for 18–24 hr. They were briefly anesthetized using CO_2 and placed into a small slit on a custom-built plastic mount at the cervix so that the head was isolated from the rest of the body. The head was then immobilized using nail polish, and the proboscis was waxed at the maxillary palps in an extended position to allow for taste solution delivery. A cover glass was placed at the base of the rostrum at a 45° angle to the plane of the plastic mount so that the proboscis was isolated from the head. The head cuticle was dissected in ice-cold adult hemolymph-like solution (AHL) lacking calcium and magnesium, the air sacs were removed, and the esophagus was severed to allow viewing of the SEZ. Calcium- and magnesium-free AHL was replaced by AHL prior to imaging.

Tastant stimulations for the MN labeling experiments and the *Mz699-Gal4* imaging were performed using an Intelligent Imaging Innovations (3i) spinning disk confocal system (40× water objective, NA = 1) with a Phasor spatial light modulator (3i) coupled to a Ti:Sapphire femtosecond laser (SpectraPhysics). Stacks of 20–23 Z-slices (1.3–1.5 µm) were obtained from the green channel at a rate of ~0.5 Hz, for both the SEZ and central brain imaging. To apply taste solutions to the proboscis, a glass pipette (with an outer diameter of 1.0 mm and an inner diameter of 0.78 mm) was filled with approximately 2 µl of taste solution using suction generated by a 1-mL syringe. The solution was drawn up the capillary slightly so that the tip of the capillary was empty. The capillary was then placed over the proboscis using a micromanipulator prior to image acquisition. At time point 5 of 20, slight pressure was applied to the syringe to deliver taste solution to the proboscis. Stimulations lasted approximately 2 s or the equivalent of one to two time points. There were 10-min intervals between successive stimulations.

MN labeling with PA-GFP

After tastant stimulation, a pre-photoactivation stack was acquired for the green and red channels. A small ROI was drawn in Slidebook (3i), and the pharyngeal and labellar nerves were scanned intermittently with 1- to 2-s bouts of 800-nm light, with an interbout delay of 5 s, to photoconvert C3PA-GFP. This procedure was continued for ~1 hr, with a 5-min break to allow for diffusion every 10 min. At the end of the labeling sequence, a post-photoactivation image stack was taken of the green and red channels.

To generate pseudo-colored images of labeled MNs, the pre-photoactivation image was subtracted from the post-photoactivation image, and the resulting stack was overlaid onto the ΔF image from the taste stimulation. The labeled neurons were pseudo-colored red, and the taste-responsive neurons were pseudo-colored green.

Two-photon calcium imaging with CsChrimson and PA-GFP photoactivation

Flies were collected at eclosion and were aged in the dark on standard fly food supplemented with all-*trans* retinal (final concentration 400 mM) for 2 to 6 days before imaging. Because 488-nm light is sufficient to activate CsChrimson, experiments using CsChrimson to activate sensory neurons were performed on a Zeiss LSM 780 NLO AxioExaminer two-photon microscope. Flies were prepared in the same manner as described above. To activate bitter-sensing neurons, a 635-nm laser (Laserglow, ~0.01 mW/mm^2) was aimed at the fly's head, which was stimulated 3-5 times (~5 s per stimulation, ~30 s between stimulations). G-CaMP was excited with 925 nm light and $\Delta F/F(\%)$ was calculated by subtracting the mean intensity of a background ROI from the mean intensity of an ROI drawn around a given G-CaMP-expressing nucleus. In most cases, responsive neurons were visually obvious and had $\Delta F/F$ values greater than 60%. To photoactivate GFP in a responding neuron, a small ROI was drawn around a single cell body and was illuminated with 760-nm light (approximately 1-1.5 μs pixel dwell time). The laser power used was between 5% and 8%, but varied from animal to animal. The photoactivation protocol was as follows: 10 baseline scans, followed by 10-15 photoactivation scans of 15 iterations each, separated by 50 baseline scans. This was repeated 3-4 times with 5-10-min rest periods between each bout of photoactivation. The extent of photoactivation was checked intermittently using 925-nm excitation. At the end of each experiment, a Z-stack that included the entire morphology of the filled neuron was acquired.

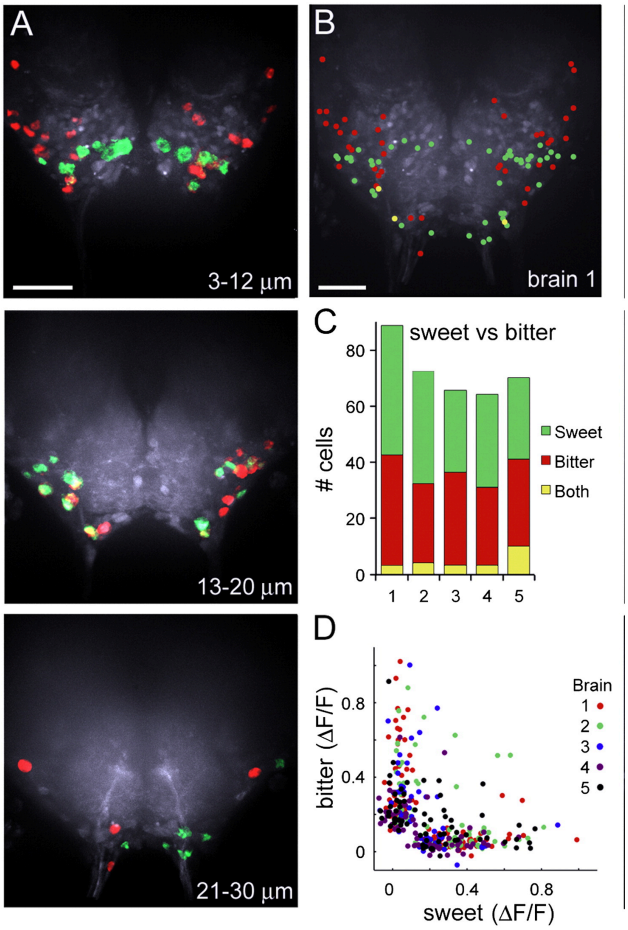


Figure 3.1: Sweet and bitter activate largely non-overlapping sets of SEZ neurons.
A. Cells responding to ATP-induced activation of proboscis bitter cells expressing P2X2 (red) and cells responding to 2 M sucrose (green). Images are maximum ΔF (representing anterior 3–12 µm, middle 13–20 µm, and posterior 21–30 µm). Scale bar, 50 µm.
B. Schematic showing all active cells in SEZ, with red representing cells activated by bitter taste cell activation and green representing cells activated by sucrose stimulation for brain shown in A. Yellow represents cells responding to bitter and sucrose stimulation (brain 1 in C). Scale bar, 50 µm.
C. Summary of responding cells for five brains. Cells responding to ATP-induced activation of GR66a bitter cells expressing P2X2 (red), cells responding to 2 M sucrose (green), and cells responding to both (yellow).
D. Plot of single-cell responses (ΔF/F) to bitter stimulations versus sucrose stimulations for brains 1–5 in (C), showing modality-selective responses.

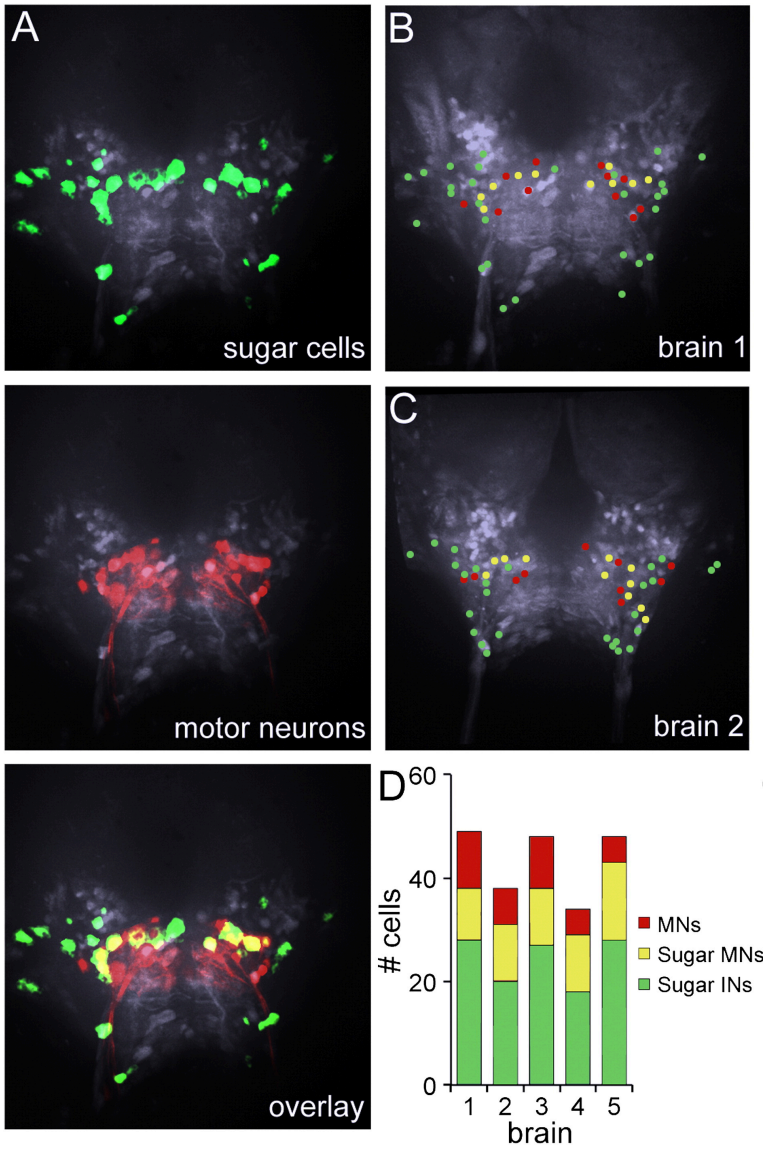


Figure 3.2: Sensory activation elicits motor responses.
A. Top: maximum ΔF of cells responding to sucrose stimulation, with cell bodies overlaid on an average max F image. Scale bar, 50 μm. Middle: MNs filled by photoactivation of C3PA-GFP in proboscis nerves (labeled red). Bottom: overlay showing the sucrose-responsive neurons that are MNs.
B. Schematic showing all active cells in SEZ, with sucrose-responsive cells not labeled by C3PA-GFP (green), sucrose-responsive MNs (yellow), and non-responsive filled MNs (red) for brain shown in A (brain 1 in D).
C. Schematic for brain 2 in (D).
D. Summary of sucrose-responsive cells not labeled by C3PA-GFP (green), sucrose-responsive MNs (yellow), and non-responsive filled MNs (red) for five brains.

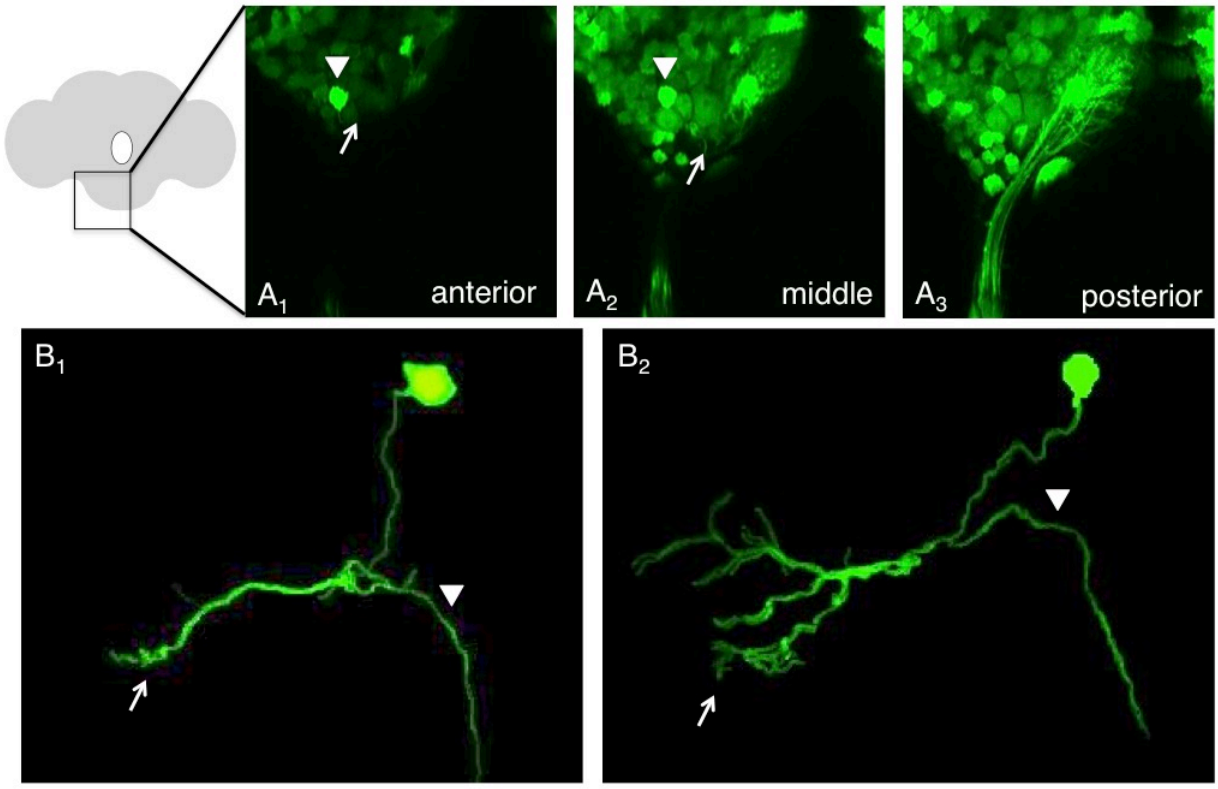


Figure 3.3: The baseline fluorescence of cytosolic GCaMP6S is too high to visualize the fine projections of the majority of PA-GFP-filled neurons.
A. Montage of a filled sugar-responsive SEZ neuron. The soma of the targeted cell (arrowheads) is brighter than the surrounding neurons, but its projection (arrows) is difficult to differentiate from the surrounding neuropil.
B. Example PA-GFP fill (B_1) of a motor neuron with its dendrites (arrow) and axon (arrowhead) leaving through the pharyngeal nerve. This fill was less successful than another (B_2), where more dendrites are visible, highlighting the variability of this protocol. In both images, surrounding fluorescence was masked for clarity.

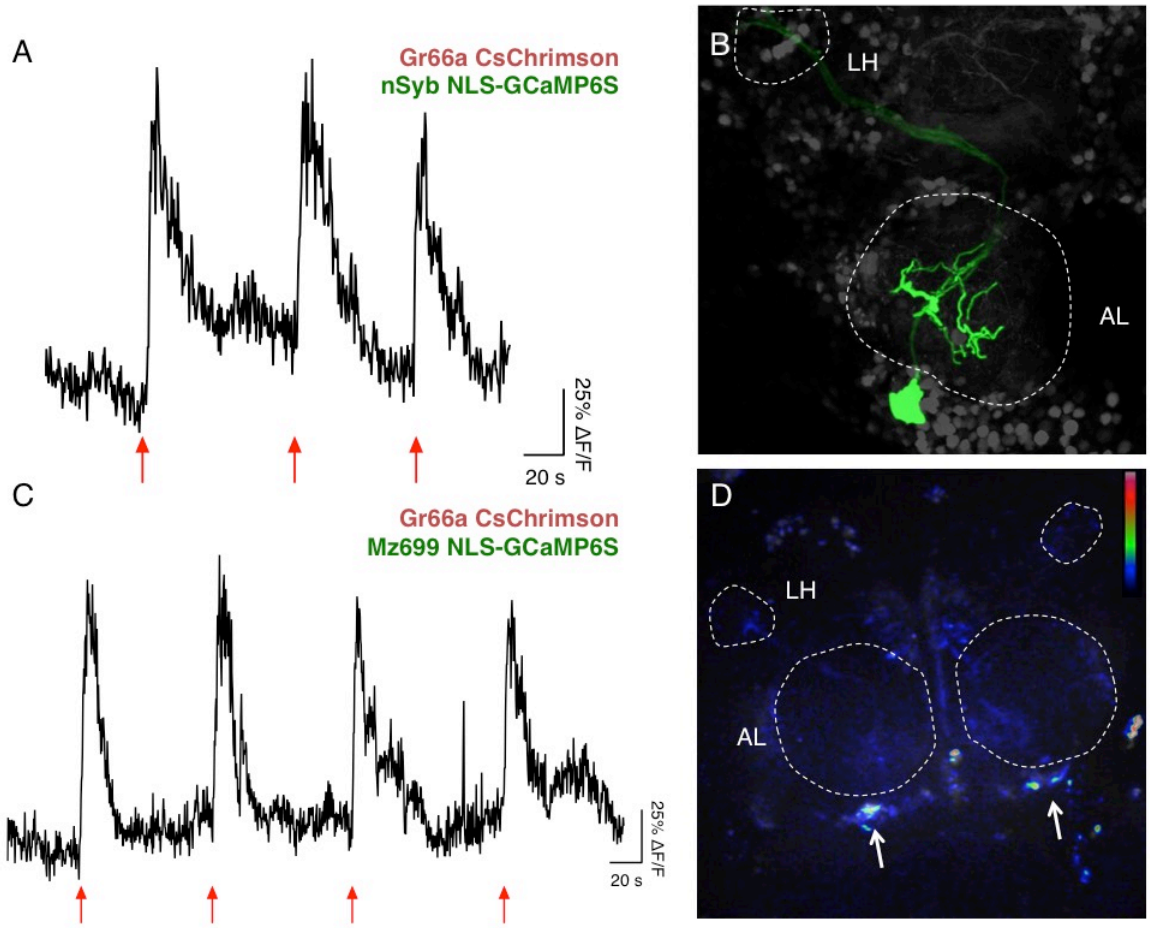


Figure 3.4: iPNs respond to bitter cell activation and natural bitter tastants.
A. Example NLS-GCaMP6S response of an SEZ neuron upon CsChrimson-mediated activation of bitter cells. This cell was located immediately ventral to the antennal lobe. Arrows indicate red laser.
B. Example PA-GFP fill of neuron in A. While more than one neuron is filled, the 5-7 filled cells all innervate the AL and project to the lateral horn.
C. Example NLS-GCaMP6S response of an Mz699-positive neuron upon CsChrimson-mediated activation of bitter cells. Arrows indicate red laser.
D. Maximum ΔF of Mz699 cells responding to stimulation with a mix of 100 mM caffeine and 10 mM denatonium. Arrows indicate iPN cell bodies.

CHAPTER 4

Discussion

These studies demonstrate that positive and negative pheromonal cues are integrated by central courtship-promoting neurons to bias a male fly's decision to mate. Using calcium imaging, I establish the existence of two populations of *fruitless*-expressing leg GRNs, one of which responds to female pheromones (F cells) and the other of which responds to male pheromones (M cells). I also show that F and M cells use different neurotransmitters and their activation either promotes or inhibits courtship, respectively.

By specifically activating each of these distinct populations while imaging the calcium response of candidate neurons in the central brain, I show that F cells activate courtship-promoting P1 neurons via PPN1, a novel class of projection neuron connecting the VNC and the protocerebrum. I also demonstrate that that both F and M cells activate mAL neurons, a class of GABAergic courtship-inhibiting neurons. Finally, using voltage imaging, I show that mAL neurons functionally inhibit P1 neurons, likely through $GABA_A$ receptors. These data suggest a model in which P1 neurons integrate multiple positive and negative pheromonal cues to compute a single decision to mate.

Nonetheless, these results do not address several important questions. In particular, how mAL neurons receive F cell inputs is unclear in the proposed model, as F cells terminate in the VNC and, unlike M cells, do no project directly to the SEZ. Another group recently showed that a class of *fruitless*-positive neurons, which they name vAB3, projects from the VNC to the SEZ and the lateral protocerebrum. By expressing P2X2 in vAB3 neurons and locally ionotophoresing ATP, the authors show that activation of vAB3 leads to calcium responses in both P1 neurons and mAL neurons, suggesting a circuit based on feedforward inhibition (Clowney et al. 2015). These data suggest that, in addition to providing an excitatory drive onto P1 neurons, PPN1 may also activate mAL neurons, as the two cell types arborize in close proximity in the SEZ. Future studies will be needed to clarify whether vAB3 is uniquely responsible for transmitting F cell activation to mAL neurons, or whether parallel circuits exist.

Why would feedforward inhibition onto P1 neurons be adaptive? Trace amounts of female pheromones likely exist in the environment but are not directly related to the presence of a virgin female. Thus, in order to prevent the untimely initiation of courtship, it is important that P1 neurons not be oversensitive to weak inputs. Inhibition by mAL neurons may act to temporally limit P1 neuron activation and maintain it within a range that keeps P1 neurons neither too sensitive nor too insensitive to female pheromones.

Many questions also remain as to whether P1 neurons integrate other pheromonal cues. Recently, it was demonstrated that a female abdomen was unable to induce a calcium response in P1 neurons until it made contact with the male's leg, suggesting that olfactory pheromones are insufficient to excite P1 neurons (at least to the level detectable by calcium imaging). Indeed, it was also observed that virgin females produced the same P1 response in males with or without their antennae but that, in contrast, mated females produced a much larger response in antenna-less males than in males with intact antennae, suggesting that inhibitory olfactory cues normally blunt P1 neuron responses to excitatory gustatory cues. In line with this, perfuming virgin females with cVA inhibited the contact-induced P1 response (Clowney et al. 2015). The identity of the neurons that transmit olfactory information to P1 neurons is unknown, as is whether P1 neurons receive input from the olfactory pathways that detect aphrodisiac volatile cues such as methyl laurate or phenylacetate.

The influence of non-chemosensory stimuli on P1 neuron activity is also incompletely understood. Recent work has shown that visual input alone—for example, moving dots—is normally insufficient to drive courtship but can trigger this behavior if P1 neurons are "primed"

by optogenetically depolarizing them (Kohatsu and Yamamoto 2015). One interpretation of these results is that input from a single modality is unable to excite P1 neurons above a "courtship threshold," and that multiple inputs are required to reach this threshold. In line with this is the observation that, unlike activation of P1 neurons, activation of F cells in the absence of a target fly does not induce courtship (data not shown).

Another unanswered question is whether all inputs to P1 neurons are equally weighted, or whether inputs from a particular modality—i.e. the gustatory or visual system—have a greater influence on P1 neuron activity. One piece of evidence to suggest that some inputs are stronger than others is that simultaneous activation of F and M cells using a PPK23 driver elicits a strong calcium response in P1 neurons. Assuming equal expression of P2X2 in F and M cells, the fact that these antagonistic inputs to P1 neurons do not simply cancel each other out implies that positive cues may carry more weight than negative ones. The specific strength of each channel could be discerned more directly by whole-cell electrophysiological recording of P1 neurons in response to F or M cell activation. This could provide a clearer picture of the inputs to which P1 neurons are most highly tuned.

The circuits downstream of P1 that control different aspects of courtship behavior also remain to be characterized. Several candidate synaptic partners have been proposed based on anatomical studies, but functional evidence of these possible connections is lacking. Similar to P1 neuron activation, activating pIP10, a class of male-specific, *fruitless*-expressing descending neuron, induced the pulse component of courtship, while silencing pIP10 greatly diminished courtship success. Based on the anatomical overlap of P1 and pIP10, it was proposed that pIP10 transmitted P1 activation to the VNC to control central pattern generators responsible for song production (von Philipsborn et al. 2011). In line with this, optogenetic activation of pIP10 induced wing extension that was strongly time-locked to the light stimulus. In contrast, activating P1 neurons led to wing extension that persisted for many minutes after offset of the light (Inagaki et al. 2014). It is unknown whether pIP10 neurons are activated by pheromones, a question that could be answered by imaging calcium responses in these neurons to ATP-mediated activation of F and M cells. In addition, calcium imaging of pIP10 neurons while optogenetically activating P1 neurons could clarify whether they are downstream of the "courtship control" center.

Interesting questions also exist with regards to the function and behavioral role of mAL neurons in the female brain. While F and M cells on the female leg respond to the same pheromones as those on the male leg, preliminary experiments that I conducted showed that simultaneous activation of F and M cells does not produce an obvious calcium response in female mAL neurons (data not shown), suggesting that the circuit logic controlling female mating behavior may be different from that of male mating behavior.

Recent studies have identified two *doublesex*-expressing neural classes in the female brain —pCd and pC1—that are crucial for female receptivity (Zhou et al. 2014). Silencing pCd or pC1 severely diminishes female receptivity, whereas activating them promotes receptivity. Both neural classes respond with calcium increases to the male-enriched pheromone cVA, while pC1 also responds to courtship song. Interestingly, simultaneous stimulation with cVA and courtship song enhances the pC1 respond to song, suggesting that pC1 neurons integrate auditory and pheromonal cues that are relevant to mating and implying that pC1 neurons in females serve an analogous function to P1 neurons in males. While the neural pathways transmitting auditory information to pC1 have been elucidated (Zhou et al. 2015), pheromonal inputs to pC1 have not been described. It will be interesting to test whether female pC1 neurons receive input from F

and/or M cells and identify the neural pathways that transmit this sensory input to the higher brain.

While many components of the courtship circuit are now known, the logic of other sensorimotor circuits remains unclear. In particular, characterization of taste circuits has lagged behind that of olfactory circuits for several reasons. First, beyond a few isolated examples, the identities of taste-responsive neurons, their morphologies, or their projection patterns are unknown. Second, the SEZ, the primary taste really in the *Drosophila* brain, is a multimodal region, making it difficult anatomically isolate taste-responsive neurons from mechanosensory-responsive or descending neurons.

Large-scale calcium imaging coupled with cell labeling is an appealing strategy to identify and label taste-responsive neurons comprehensively and in an unbiased manner. By driving the expression of G-CaMP and PA-GFP pan-neuronally, it is possible to visualize the entire complement of taste-responsive neurons and then label individual cells. In an ideal scenario, one would then be able to identify a filled neuron in a Gal4 driver line, which could then be used to activate, silence, or otherwise manipulate that neuron to test its role in behavior or identify upstream or downstream partners.

Nevertheless, filling single taste-responsive SEZ neurons has been challenging for several reasons. First, it has been difficult to target single neurons without photoconverting PA-GFP in neighboring cells as well. This is unequivocally due to movement inherent to the *in vivo* preparation. To circumvent this issue, I attempted to image SEZ G-CaMP responses to bitter or sugar cell activation in a brain explant but was unable to observe more than a few responding neurons (compared to the ~35 neurons observed in the *in vivo* preparation) (Harris et al. 2015). Another potential strategy to lessen movement in the *in vivo* preparation is to paralyze the fly after identifying a taste-responsive neuron but before filling it. This could be accomplished by using philanthotoxin, a glutamate receptor antagonist routinely used in studies of the larval neuromuscular junction. Future studies will be necessary to test the effectiveness of this approach.

A second obstacle is that the quality of filling appears to depend on the particular neuron that is targeted. Larger neurons appear to fill more readily, likely because of higher concentrations of PA-GFP. The cell bodies of smaller neurons do become extremely bright, and, in general, it is possible to trace a neurite projecting away from the cell body from some distance. Nonetheless, tracing fibers to their complete extent is usually not possible. This may be because the diffusion of PA-GFP through narrow neurites is poor. Alternatively, the issue may be low signal-to-noise of photoconverted PA-GFP against a background of pan-neuronal baseline PA-GFP fluorescence. Performing these experiments on newer, higher-resolution microscopes, which are only now coming online, may solve this issue.

Third, many of these problems may be inherent to the SEZ. Gustatory sensory projections appear to express PA-GFP at high levels, making it difficult to trace filled neurites that travel above or close to them. Driving expression of Gal80 in bitter or sugar sensory neurons in order to suppress expression of PA-GFP may alleviate this problem.

While several technical hurdles remain, in its current form this approach is still quite powerful and can provide unexpected insights, for example the finding that a subset of olfactory neurons responds to bitter tastants and thus may in fact be multimodal. Optimization of the photoactivation protocol, along with improved microscopes, will likely make it possible to target single neurons, visualize their morphology, and interrogate their function.

References

Agrawal, Sweta, Steve Safarik, and Michael Dickinson. 2014. "The Relative Roles of Vision and Chemosensation in Mate Recognition of Drosophila Melanogaster." *The Journal of Experimental Biology* 217 (Pt 15): 2796–2805. doi:10.1242/jeb.105817.

Baek, Myungin, Jonathan Enriquez, and Richard S Mann. 2013. "Dual Role for Hox Genes and Hox Co-Factors in Conferring Leg Motoneuron Survival and Identity in Drosophila." *Development (Cambridge, England)* 140 (9): 2027–38. doi:10.1242/dev.090902.

Billeter, Jean-Christophe, Jade Atallah, Joshua J Krupp, Jocelyn G Millar, and Joel D Levine. 2009. "Specialized Cells Tag Sexual and Species Identity in Drosophila Melanogaster." *Nature* 461 (7266): 987–91. doi:10.1038/nature08495.

Billeter, Jean-Christophe, Elizabeth J Rideout, Anthony J Dornan, and Stephen F Goodwin. 2006. "Control of Male Sexual Behavior in Drosophila by the Sex Determination Pathway." *Current Biology* 16 (17): R766–76. doi:10.1016/j.cub.2006.08.025.

Bray, Steven, and Hubert Amrein. 2003. "A Putative Drosophila Pheromone Receptor Expressed in Male-Specific Taste Neurons Is Required for Efficient Courtship." *Neuron* 39 (6): 1019–29. doi:10.1016/S0896-6273(03)00542-7.

Cachero, Sebastian, Aaron D Ostrovsky, Jai Y Yu, Barry J Dickson, and Gregory S X E Jefferis. 2010a. "Sexual Dimorphism in the Fly Brain." *Current Biology : CB* 20 (18). Elsevier Ltd: 1589–1601. doi:10.1016/j.cub.2010.07.045.

Cachero, Sebastian, Aaron D. Ostrovsky, Jai Y. Yu, Barry J. Dickson, and G. S X E Jefferis. 2010b. "Sexual Dimorphism in the Fly Brain." *Current Biology* 20 (18): 1589–1601. doi:10.1016/j.cub.2010.07.045.

Cao, Guan, Jelena Platisa, Vincent A. Pieribone, Davide Raccuglia, Michael Kunst, and Michael N. Nitabach. 2013. "Genetically Targeted Optical Electrophysiology in Intact Neural Circuits." *Cell* 154 (4): 904–13. doi:10.1016/j.cell.2013.07.027.

Chamero, Pablo, Tobias F Marton, Darren W Logan, Kelly Flanagan, Jason R Cruz, Alan Saghatelian, Benjamin F Cravatt, and Lisa Stowers. 2007. "Identification of Protein Pheromones That Promote Aggressive Behaviour." *Nature* 450 (7171): 899–902. doi:10.1038/nature05997.

Chen, Tsai-Wen, Trevor J Wardill, Yi Sun, Stefan R Pulver, Sabine L Renninger, Amy Baohan, Eric R Schreiter, et al. 2013. "Ultrasensitive Fluorescent Proteins for Imaging Neuronal Activity." *Nature* 499 (7458): 295–300. doi:10.1038/nature12354.

Chen, X., M. Gabitto, Y. Peng, N. J. P. Ryba, and C. S. Zuker. 2011. "A Gustotopic Map of Taste Qualities in the Mammalian Brain." *Science* 333 (6047): 1262–66. doi:10.1126/science.1204076.

Cline, T. W. 1978. "Two Closely Linked Mutations in Drosophila Melanogaster That Are Lethal to Opposite Sexes and Interact with Daughterless." *Genetics* 90 (4): 683–97.

Clowney, E. Josephine, Shinya Iguchi, Jennifer J. Bussell, Elias Scheer, and Vanessa Ruta. 2015. "Multimodal Chemosensory Circuits Controlling Male Courtship in Drosophila." *Neuron* 87 (5): 1036–49. doi:10.1016/j.neuron.2015.07.025.

Coen, Philip, and Mala Murthy. 2016. "Singing on the Fly: Sensorimotor Integration and Acoustic Communication in Drosophila." *Current Opinion in Neurobiology*. doi:10.1016/j.conb.2016.01.013.

Daniels, Richard W., Maria V. Gelfand, Catherine A. Collins, and Aaron DiAntonio. 2008. "Visualizing Glutamatergic Cell Bodies and Synapses in Drosophila Larval and Adult

CNS." *Journal of Comparative Neurology* 508 (1): 131–52. doi:10.1002/cne.21670.
Datta, Sandeep Robert, Maria Luisa Vasconcelos, Vanessa Ruta, Sean Luo, Allan Wong, Ebru Demir, Jorge Flores, Karen Balonze, Barry J Dickson, and Richard Axel. 2008. "The Drosophila Pheromone cVA Activates a Sexually Dimorphic Neural Circuit." *Nature* 452 (7186): 473–77. doi:10.1038/nature06808.
Demir, Ebru, and Barry J. Dickson. 2005. "Fruitless Splicing Specifies Male Courtship Behavior in Drosophila." *Cell* 121 (5): 785–94. doi:10.1016/j.cell.2005.04.027.
Diao, Fengqiu, Holly Ironfield, Haojiang Luan, Feici Diao, William C. Shropshire, John Ewer, Elizabeth Marr, Christopher J. Potter, Matthias Landgraf, and Benjamin H. White. 2015. "Plug-and-Play Genetic Access to Drosophila Cell Types Using Exchangeable Exon Cassettes." *Cell Reports* 10 (8): 1410–21. doi:10.1016/j.celrep.2015.01.059.
Dulac, Catherine, and a Thomas Torello. 2003. "Molecular Detection of Pheromone Signals in Mammals: From Genes to Behaviour." *Nature Reviews. Neuroscience* 4 (7): 551–62. doi:10.1038/nrn1140.
Dweck, Hany K M, Shimaa A M Ebrahim, Michael Thoma, Ahmed A M Mohamed, Ian W Keesey, Federica Trona, Sofia Lavista-Llanos, et al. 2015. "Pheromones Mediating Copulation and Attraction in Drosophila." *Proceedings of the National Academy of Sciences of the United States of America* 112 (21): E2829–35. doi:10.1073/pnas.1504527112.
Ejima, Aki, and Leslie C Griffith. 2008. "Courtship Initiation Is Stimulated by Acoustic Signals in Drosophila Melanogaster." *PloS One* 3 (9): e3246. doi:10.1371/journal.pone.0003246.
Ferveur, Jean François. 2005. "Cuticular Hydrocarbons: Their Evolution and Roles in Drosophila Pheromonal Communication." *Behavior Genetics*. doi:10.1007/s10519-005-3220-5.
Ffrench-Constant, R H, D P Mortlock, C D Shaffer, R J MacIntyre, and R T Roush. 1991. "Molecular Cloning and Transformation of Cyclodiene Resistance in Drosophila: An Invertebrate Gamma-Aminobutyric Acid Subtype A Receptor Locus." *Proceedings of the National Academy of Sciences of the United States of America* 88 (16): 7209–13. doi:10.1073/pnas.89.16.7849b.
Flood, Thomas F., Shinya Iguchi, Michael Gorczyca, Benjamin White, Kei Ito, and Motojiro Yoshihara. 2013. "A Single Pair of Interneurons Commands the Drosophila Feeding Motor Program." *Nature* 499 (7456): 83–87. doi:10.1038/nature12208.
Fu, Xiaoyan, Yuetian Yan, Pei S. Xu, Ilan Geerlof-Vidavsky, Wongi Chong, Michael L. Gross, and Timothy E. Holy. 2015. "A Molecular Code for Identity in the Vomeronasal System." *Cell* 163 (2): 313–23. doi:10.1016/j.cell.2015.09.012.
Gohl, Daryl M, Marion a Silies, Xiaojing J Gao, Sheetal Bhalerao, Francisco J Luongo, Chun-Chieh Lin, Christopher J Potter, and Thomas R Clandinin. 2011. "A Versatile in Vivo System for Directed Dissection of Gene Expression Patterns." *Nature Methods* 8 (3): 231–37. doi:10.1038/nmeth.1561.
Gordon, Michael D, and Kristin Scott. 2009. "Motor Control in a Drosophila Taste Circuit." *Neuron*, 373–84. doi:10.1016/j.neuron.2008.12.033.
Grosjean, Yael, Raphael Rytz, Jean-pierre Farine, Liliane Abuin, Jérôme Cortot, Gregory S. X. E. Jefferis, and Richard Benton. 2011. "An Olfactory Receptor for Food-Derived Odours Promotes Male Courtship in Drosophila." *Nature* 478 (7368): 236–40. doi:10.1038/nature10428.
Ha, Tal Soo, and Dean P Smith. 2006. "A Pheromone Receptor Mediates 11-Cis-Vaccenyl Acetate-Induced Responses in Drosophila." *Journal of Neuroscience* 26 (34): 8727–33. doi:10.1523/jneurosci.0876-06.2006.

Haga-Yamanaka, Sachiko, Limei Ma, Jie He, Qiang Qiu, Luke D. Lavis, Loren L. Looger, and C. Ron Yu. 2014. "Integrated Action of Pheromone Signals in Promoting Courtship Behavior in Male Mice." *eLife* 2014 (3). doi:10.7554/eLife.03025.001.

Hamada, Fumika N, Mark Rosenzweig, Kyeongjin Kang, Stefan R Pulver, Alfredo Ghezzi, Timothy J Jegla, and Paul a Garrity. 2008. "An Internal Thermal Sensor Controlling Temperature Preference in Drosophila." *Nature* 454 (7201): 217–20. doi:10.1038/nature07001.

Hampel, Stefanie, Romain Franconville, Julie H. Simpson, and Andrew M. Seeds. 2015. "A Neural Command Circuit for Grooming Movement Control." *eLife* 4 (September). doi:10.7554/eLife.08758.

Han, DD D, D Stein, and LM M Stevens. 2000. "Investigating the Function of Follicular Subpopulations during Drosophila Oogenesis through Hormone-Dependent Enhancer-Targeted Cell Ablation." *Development {(Cambridge,} England)* 127 (3): 573–83. http://www.ncbi.nlm.nih.gov/pubmed/10631178\nhttp://dev.biologists.org/content/127/3/573.short.

Harris, David T., Benjamin R. Kallman, Brendan C. Mullaney, and Kristin Scott. 2015. "Representations of Taste Modality in the Drosophila Brain." *Neuron* 86 (6): 1449–60. doi:10.1016/j.neuron.2015.05.026.

Hsu, Cynthia T, and Vikas Bhandawat. 2016. "Organization of Descending Neurons in Drosophila Melanogaster." *Scientific Reports* 6: 20259. doi:10.1038/srep20259.

Inagaki, Hidehiko K, Yonil Jung, Eric D Hoopfer, Allan M Wong, Neeli Mishra, John Y Lin, Roger Y Tsien, and David J Anderson. 2014. "Optogenetic Control of Drosophila Using a Red-Shifted Channelrhodopsin Reveals Experience-Dependent Influences on Courtship." *Nature Methods* 11 (3): 325–32. doi:10.1038/nmeth.2765.

Ito, Hiroki, Kosei Sato, Masayuki Koganezawa, Manabu Ote, Ken Matsumoto, Chihiro Hama, and Daisuke Yamamoto. 2012. "Fruitless Recruits Two Antagonistic Chromatin Factors to Establish Single-Neuron Sexual Dimorphism." *Cell* 149 (6): 1327–38. doi:10.1016/j.cell.2012.04.025.

Jenett, Arnim, Gerald M. Rubin, Teri T B Ngo, David Shepherd, Christine Murphy, Heather Dionne, Barret D. Pfeiffer, et al. 2012. "A GAL4-Driver Line Resource for Drosophila Neurobiology." *Cell Reports* 2 (4): 991–1001. doi:10.1016/j.celrep.2012.09.011.

Juntti, Scott A., Jessica Tollkuhn, Melody V. Wu, Eleanor J. Fraser, Taylor Soderborg, Stella Tan, Shin Ichiro Honda, Nobuhiro Harada, and Nirao M. Shah. 2010. "The Androgen Receptor Governs the Execution, but Not Programming, of Male Sexual and Territorial Behaviors." *Neuron* 66 (2): 260–72. doi:10.1016/j.neuron.2010.03.024.

Kankel, Douglas R., and Jeffrey C. Hall. 1976. "Fate Mapping of Nervous System and Other Internal Tissues in Genetic Mosaics of Drosophila Melanogaster." *Developmental Biology* 48 (1): 1–24. doi:10.1016/0012-1606(76)90041-5.

Kimura, K I, M Ote, T Tazawa, and D Yamamoto. 2005. "Fruitless Specifies Sexually Dimorphic Neural Circuitry in the Drosophila Brain." *Nature* 438 (7065): 229–33. doi:10.1038/nature04229.

Kimura, Ken ichi, Tomoaki Hachiya, Masayuki Koganezawa, Tatsunori Tazawa, and Daisuke Yamamoto. 2008. "Fruitless and Doublesex Coordinate to Generate Male-Specific Neurons That Can Initiate Courtship." *Neuron* 59 (5): 759–69. doi:10.1016/j.neuron.2008.06.007.

Klapoetke, Nathan C, Yasunobu Murata, Sung Soo Kim, Stefan R Pulver, Amanda Birdsey-Benson, Yong Ku Cho, Tania K Morimoto, et al. 2014. "Independent Optical Excitation of

Distinct Neural Populations." *Nature Methods* 11 (3): 338–46. doi:10.1038/nmeth.2836.
Koganezawa, Masayuki, Ken ichi Kimura, and Daisuke Yamamoto. 2016. "The Neural Circuitry That Functions as a Switch for Courtship versus Aggression in Drosophila Males." *Current Biology* 26 (11): 1395–1403. doi:10.1016/j.cub.2016.04.017.
Koganezawa, Masayuki, Takashi Matsuo, Ken Ichi Kimura, and Daisuke Yamamoto. 2009. "Shaping of Drosophila Male Courtship Posture by a Gustatory Pheromone." In *Annals of the New York Academy of Sciences*, 1170:497–501. doi:10.1111/j.1749-6632.2009.03889.x.
Koh, Tong Wey, Zhe He, Srinivas Gorur-Shandilya, Karen Menuz, Nikki K. Larter, Shannon Stewart, and John R. Carlson. 2014. "The Drosophila IR20a Clade of Ionotropic Receptors Are Candidate Taste and Pheromone Receptors." *Neuron* 83 (4): 850–65. doi:10.1016/j.neuron.2014.07.012.
Kohatsu, Soh, Masayuki Koganezawa, and Daisuke Yamamoto. 2011. "Female Contact Activates Male-Specific Interneurons That Trigger Stereotypic Courtship Behavior in Drosophila." *Neuron* 69 (3): 498–508. doi:10.1016/j.neuron.2010.12.017.
Kohatsu, Soh, and Daisuke Yamamoto. 2015. "Visually Induced Initiation of Drosophila Innate Courtship-like Following Pursuit Is Mediated by Central Excitatory State." *Nature Communications* 6: 6457. doi:10.1038/ncomms7457.
Kohl, Johannes, Aaron D. Ostrovsky, Shahar Frechter, and Gregory S X E Jefferis. 2013. "A Bidirectional Circuit Switch Reroutes Pheromone Signals in Male and Female Brains." *Cell* 155 (7): 1610–23. doi:10.1016/j.cell.2013.11.025.
Krstic, Dimitrije, Werner Boll, and Markus Noll. 2009. "Sensory Integration Regulating Male Courtship Behavior in Drosophila." *PLoS ONE* 4 (2). doi:10.1371/journal.pone.0004457.
Kurtovic, Amina, Alexandre Widmer, and Barry J Dickson. 2007. "A Single Class of Olfactory Neurons Mediates Behavioural Responses to a Drosophila Sex Pheromone." *Nature* 446 (7135): 542–46. doi:10.1038/nature05672.
Lai, Sen-Lin, Takeshi Awasaki, Kei Ito, and Tzumin Lee. 2008. "Clonal Analysis of Drosophila Antennal Lobe Neurons: Diverse Neuronal Architectures in the Lateral Neuroblast Lineage." *Development (Cambridge, England)* 135 (17): 2883–93. doi:10.1242/dev.024380.
Lai, Sen-Lin, and Tzumin Lee. 2006. "Genetic Mosaic with Dual Binary Transcriptional Systems in Drosophila." *Nature Neuroscience* 9 (5): 703–9. doi:10.1038/nn1681.
Lee, Gyunghee, Jeffrey C Hall, and Jae H Park. 2002. "Doublesex Gene Expression in the Central Nervous System of Drosophila Melanogaster." *Journal of Neurogenetics* 16 (4): 229–48. doi:10.1080/01677060216292.
Liang, Liang, Yulong Li, ChristopherJ Potter, Ofer Yizhar, Karl Deisseroth, RichardW Tsien, and Liqun Luo. 2013. "GABAergic Projection Neurons Route Selective Olfactory Inputs to Specific Higher-Order Neurons." *Neuron* 79 (5): 917–31. doi:10.1016/j.neuron.2013.06.014.
Lima, Susana Q., and Gero Miesenböck. 2005. "Remote Control of Behavior through Genetically Targeted Photostimulation of Neurons." *Cell* 121 (1): 141–52. doi:10.1016/j.cell.2005.02.004.
Liu, Weiwei, Xinhua Liang, Jianxian Gong, Zhen Yang, Yao-Hua Zhang, Jian-Xu Zhang, and Yi Rao. 2011. "Social Regulation of Aggression by Pheromonal Activation of Or65a Olfactory Neurons in Drosophila." *Nature Neuroscience* 14 (7). Nature Publishing Group: 896–902. doi:10.1038/nn.2836.
Lu, Beika, Angela LaMora, Yishan Sun, Michael J. Welsh, and Yehuda Ben-Shahar. 2012. "Ppk23-Dependent Chemosensory Functions Contribute to Courtship Behavior in

Drosophila Melanogaster." *PLoS Genetics* 8 (3). doi:10.1371/journal.pgen.1002587.
Manoli, Devanand S, Margit Foss, Adriana Villella, Barbara J Taylor, Jeffrey C Hall, and Bruce S Baker. 2005. "Male-Specific Fruitless Specifies the Neural Substrates of Drosophila Courtship Behaviour." *Nature* 436 (7049): 395–400. doi:10.1038/nature03859.
Manoli, Devanand S., Pu Fan, Eleanor J. Fraser, and Nirao M. Shah. 2013. "Neural Control of Sexually Dimorphic Behaviors." *Current Opinion in Neurobiology*. doi:10.1016/j.conb.2013.04.005.
Manzo, A., M. Silies, D. M. Gohl, and K. Scott. 2012. "Motor Neurons Controlling Fluid Ingestion in Drosophila." *Proceedings of the National Academy of Sciences* 109 (16): 6307–12. doi:10.1073/pnas.1120305109.
Mellert, David J, Jon-Michael Knapp, Devanand S Manoli, Geoffrey W Meissner, and Bruce S Baker. 2010. "Midline Crossing by Gustatory Receptor Neuron Axons Is Regulated by Fruitless, Doublesex and the Roundabout Receptors." *Development (Cambridge, England)* 137 (2): 323–32. doi:10.1242/dev.045047.
Miyamoto, Tetsuya, and Hubert Amrein. 2008. "Suppression of Male Courtship by a Drosophila Pheromone Receptor." *Nature Neuroscience* 11 (8): 874–76. doi:10.1038/nn.2161.
Moon, Seok Jun, Youngseok Lee, Yuchen Jiao, and Craig Montell. 2009. "A Drosophila Gustatory Receptor Essential for Aversive Taste and Inhibiting Male-to-Male Courtship." *Current Biology* 19 (19): 1623–27. doi:10.1016/j.cub.2009.07.061.
Nicolai, L. J. J., A. Ramaekers, T. Raemaekers, A. Drozdzecki, A. S. Mauss, J. Yan, M. Landgraf, W. Annaert, and B. A. Hassan. 2010. "Genetically Encoded Dendritic Marker Sheds Light on Neuronal Connectivity in Drosophila." *Proceedings of the National Academy of Sciences* 107 (47): 20553–58. doi:10.1073/pnas.1010198107.
Ogawa, S, D B Lubahn, K S Korach, and D W Pfaff. 1997. "Behavioral Effects of Estrogen Receptor Gene Disruption in Male Mice." *Proceedings of the National Academy of Sciences of the United States of America* 94 (4): 1476–81. doi:10.1073/pnas.94.4.1476.
Pan, Y., G. W. Meissner, and B. S. Baker. 2012. "Joint Control of Drosophila Male Courtship Behavior by Motion Cues and Activation of Male-Specific P1 Neurons." *Proceedings of the National Academy of Sciences* 109 (25): 10065–70. doi:10.1073/pnas.1207107109.
Parnas, Moshe, AndrewC Lin, Wolf Huetteroth, and Gero Miesenböck. 2013. "Odor Discrimination in Drosophila: From Neural Population Codes to Behavior." *Neuron* 79 (5): 932–44. doi:10.1016/j.neuron.2013.08.006.
Pauli, Andrea, Friederike Althoff, Raquel A. Oliveira, Stefan Heidmann, Oren Schuldiner, Christian F. Lehner, Barry J. Dickson, and Kim Nasmyth. 2008. "Cell-Type-Specific TEV Protease Cleavage Reveals Cohesin Functions in Drosophila Neurons." *Developmental Cell* 14 (2): 239–51. doi:10.1016/j.devcel.2007.12.009.
Penalva, Luiz O F, and Lucas Sánchez. 2003. "RNA Binding Protein Sex-Lethal (Sxl) and Control of Drosophila Sex Determination and Dosage Compensation." *Microbiology and Molecular Biology Reviews : MMBR* 67 (3): 343–59 – table of contents. doi:10.1128/MMBR.67.3.343–359.2003.
Pfeiffer, B. D., T.-T. B. Ngo, K. L. Hibbard, C. Murphy, A. Jenett, J. W. Truman, and G. M. Rubin. 2010. "Refinement of Tools for Targeted Gene Expression in Drosophila." *Genetics* 186 (2): 735–55. doi:10.1534/genetics.110.119917.
Pfeiffer, B. D., J. W. Truman, and G. M. Rubin. 2012. "Using Translational Enhancers to Increase Transgene Expression in Drosophila." *Proceedings of the National Academy of Sciences* 109 (17): 6626–31. doi:10.1073/pnas.1204520109.

Pikielny, Claudio W. 2012. “Sexy DEG/ENaC Channels Involved in Gustatory Detection of Fruit Fly Pheromones.” *Science Signaling* 5 (249): pe48. doi:10.1126/scisignal.2003555.
Rajashekhar, K. P., and R. N. Singh. 1994. “Organization of Motor Neurons Innervating the Proboscis Musculature in Drosophila Melanogaster Meigen (Diptera : Drosophilidae).” *International Journal of Insect Morphology and Embryology* 23 (3): 225–42. doi:10.1016/0020-7322(94)90020-5.
Roberts, Sarah A, Deborah M Simpson, Stuart D Armstrong, Amanda J Davidson, Duncan H Robertson, Lynn McLean, Robert J Beynon, and Jane L Hurst. 2010. “Darcin: A Male Pheromone That Stimulates Female Memory and Sexual Attraction to an Individual Male’s Odour.” *BMC Biology* 8: 75. doi:10.1186/1741-7007-8-75.
Ruta, Vanessa, Sandeep Robert Datta, Maria Luisa Vasconcelos, Jessica Freeland, Loren L Looger, and Richard Axel. 2010. “A Dimorphic Pheromone Circuit in Drosophila from Sensory Input to Descending Output.” *Nature* 468 (7324): 686–90. doi:10.1038/nature09554.
Salz, Helen K., and James W. Erickson. 2010. “Sex Determination in Drosophila: The View from the Top.” *Fly* 4 (1): 60–70. doi:10.4161/fly.4.1.11277.
Sokolowski, M B. 2001. “Drosophila: Genetics Meets Behaviour.” *Nature Reviews. Genetics* 2 (11): 879–90. doi:10.1038/35098592.
Starostina, Elena, Tong Liu, Vinoy Vijayan, Zheng Zheng, Kathleen K Siwicki, and Claudio W Pikielny. 2012. “A Drosophila DEG/ENaC Subunit Functions Specifically in Gustatory Neurons Required for Male Courtship Behavior.” *The Journal of Neuroscience : The Official Journal of the Society for Neuroscience* 32 (13): 4665–74. doi:10.1523/JNEUROSCI.6178-11.2012.
Stocker, R. F. 1994. “The Organization of the Chemosensory System in Drosophila Melanogaster: A Review.” *Cell and Tissue Research*. doi:10.1007/BF00305372.
Stockinger, Petra, Duda Kvitsiani, Shay Rotkopf, L??szl?? Tiri??n, and Barry J. Dickson. 2005. “Neural Circuitry That Governs Drosophila Male Courtship Behavior.” *Cell* 121 (5): 795–807. doi:10.1016/j.cell.2005.04.026.
Stowers, Lisa, and Stephen D. Liberles. 2016. “State-Dependent Responses to Sex Pheromones in Mouse.” *Current Opinion in Neurobiology*. doi:10.1016/j.conb.2016.04.001.
Strutz, Antonia, Jan Soelter, Amelie Baschwitz, Abu Farhan, Veit Grabe, Jürgen Rybak, Markus Knaden, Michael Schmuker, Bill S. Hansson, and Silke Sachse. 2014. “Decoding Odor Quality and Intensity in the Drosophila Brain.” *eLife* 3: e04147. doi:10.7554/eLife.04147.
Tanaka, Nobuaki K., Keita Endo, and Kei Ito. 2012. “Organization of Antennal Lobe-Associated Neurons in Adult Drosophila Melanogaster Brain.” *Journal of Comparative Neurology* 520 (18): 4067–4130. doi:10.1002/cne.23142.
Thistle, Robert, Peter Cameron, Azeen Ghorayshi, Lisa Dennison, and Kristin Scott. 2012. “Contact Chemoreceptors Mediate Male-Male Repulsion and Male-Female Attraction during Drosophila Courtship.” *Cell* 149 (5). Elsevier Inc.: 1140–51. doi:10.1016/j.cell.2012.03.045.
Tinbergen, N. 1952. “The Curious Behavior of the Stickleback.” *Scientific American*. doi:10.1038/scientificamerican1252-22.
Tinbergen, N., and A.C. C Perdeck. 1950. “On the Stimulus Situation Releasing the Begging Response in the Newly Hatched Herring Gull Chick (Larus A. Argentatus Pont.).” *Behaviour* 3 (1): 1–39. doi:10.1163/156853951X00197.
Toda, Hirofumi, Xiaoliang Zhao, and Barry J. Dickson. 2012. “The Drosophila Female

Aphrodisiac Pheromone Activates ppk23+ Sensory Neurons to Elicit Male Courtship Behavior." *Cell Reports*, May. The Authors, 1–9. doi:10.1016/j.celrep.2012.05.007.
Toda, K., Okada T, K. Takeda, S. Akira, T. Saibara, M. Shiraishi, S. Onishi, and Y. Shizuta. 2001. "Oestrogen at the Neonatal Stage Is Critical for the Reproductive Ability of Male Mice as Revealed by Supplementation with 17??-Oestradiol to Aromatase Gene (Cyp19) Knockout Mice." *Journal of Endocrinology* 168 (3): 455–63. doi:10.1677/joe.0.1680455.
Toda, K., T. Saibara, T. Okada, S. Onishi, and Y. Shizuta. 2001. "A Loss of Aggressive Behaviour and Its Reinstatement by Oestrogen in Mice Lacking the Aromatase Gene (Cyp19)." *Journal of Endocrinology* 168 (2): 217–20. doi:10.1677/joe.0.1680217.
Unger, Elizabeth K., Kenneth J. Burke, Cindy F. Yang, Kevin J. Bender, Patrick M. Fuller, and Nirao M. Shah. 2015. "Medial Amygdalar Aromatase Neurons Regulate Aggression in Both Sexes." *Cell Reports* 10 (4): 453–63. doi:10.1016/j.celrep.2014.12.040.
Venken, Koen J T, Yuchun He, Roger a Hoskins, and Hugo J Bellen. 2006. "P[acman]: A BAC Transgenic Platform for Targeted Insertion of Large DNA Fragments in D. Melanogaster." *Science (New York, N.Y.)* 314 (5806): 1747–51. doi:10.1126/science.1134426.
Vijayan, Vinoy, Rob Thistle, Tong Liu, Elena Starostina, and Claudio W. Pikielny. 2014. "Drosophila Pheromone-Sensing Neurons Expressing the ppk25 Ion Channel Subunit Stimulate Male Courtship and Female Receptivity." *PLoS Genetics* 10 (3). doi:10.1371/journal.pgen.1004238.
von Philipsborn, Anne C., Tianxiao Liu, Jai Y. Yu, Christopher Masser, Salil S. Bidaye, and Barry J. Dickson. 2011. "Neuronal Control of Drosophila Courtship Song." *Neuron* 69 (3): 509–22. doi:10.1016/j.neuron.2011.01.011.
von Schlichet, Florian, and Jeffrey C. Hall. 1979. "Neural Topography of Courtship Song in Sex Mosaics of Drosophila Melanogaster." *Journal of Comparative Physiology ??? A* 129 (1): 85–95. doi:10.1007/BF00679915.
Wang, Jing W., Allan M. Wong, Jorge Flores, Leslie B. Vosshall, and Richard Axel. 2003. "Two-Photon Calcium Imaging Reveals an Odor-Evoked Map of Activity in the Fly Brain." *Cell* 112 (2): 271–82. doi:10.1016/S0092-8674(03)00004-7.
Wang, Liming, and David J Anderson. 2010. "Identification of an Aggression-Promoting Pheromone and Its Receptor Neurons in Drosophila." *Nature* 463 (7278): 227–31. doi:10.1038/nature08678.
Wang, Liming, Xiaoqing Han, Jennifer Mehren, Makoto Hiroi, Jean-Christophe Billeter, Tetsuya Miyamoto, Hubert Amrein, Joel D Levine, and David J Anderson. 2011. "Hierarchical Chemosensory Regulation of Male-Male Social Interactions in Drosophila." *Nature Neuroscience* 14 (6): 757–62. doi:10.1038/nn.2800.
Wang, Zuoren, Aakanksha Singhvi, Priscilla Kong, and Kristin Scott. 2004. "Taste Representations in the Drosophila Brain." *Cell* 117 (7): 981–91. doi:10.1016/j.cell.2004.06.011.
Watanabe, Kanako, Gakuta Toba, Masayuki Koganezawa, and Daisuke Yamamoto. 2011. "Gr39a, a Highly Diversified Gustatory Receptor in Drosophila, Has a Role in Sexual Behavior." *Behavior Genetics* 41 (5): 746–53. doi:10.1007/s10519-011-9461-6.
Wu, Melody V., Devanand S. Manoli, Eleanor J. Fraser, Jennifer K. Coats, Jessica Tollkuhn, Shin Ichiro Honda, Nobuhiro Harada, and Nirao M. Shah. 2009. "Estrogen Masculinizes Neural Pathways and Sex-Specific Behaviors." *Cell* 139 (1): 61–72. doi:10.1016/j.cell.2009.07.036.
Wu, Melody V., and Nirao M. Shah. 2011. "Control of Masculinization of the Brain and

Behavior." *Current Opinion in Neurobiology*. doi:10.1016/j.conb.2010.09.014.
Yamamoto, Daisuke, Kosei Sato, and Masayuki Koganezawa. 2014. "Neuroethology of Male Courtship in Drosophila: From the Gene to Behavior." *Journal of Comparative Physiology A: Neuroethology, Sensory, Neural, and Behavioral Physiology*. doi:10.1007/s00359-014-0891-5.
Yang, Cindy F., Michael C. Chiang, Daniel C. Gray, Mahalakshmi Prabhakaran, Maricruz Alvarado, Scott A. Juntti, Elizabeth K. Unger, James A. Wells, and Nirao M. Shah. 2013. "Sexually Dimorphic Neurons in the Ventromedial Hypothalamus Govern Mating in Both Sexes and Aggression in Males." *Cell* 153 (4): 896–909. doi:10.1016/j.cell.2013.04.017.
Yao, Z., A. M. Macara, K. R. Lelito, T. Y. Minosyan, and O. T. Shafer. 2012. "Analysis of Functional Neuronal Connectivity in the Drosophila Brain." *Journal of Neurophysiology* 108 (2): 684–96. doi:10.1152/jn.00110.2012.
Yapici, Nilay, Raphael Cohn, Christian Schusterreiter, Vanessa Ruta, and Leslie B. Vosshall. 2016. "A Taste Circuit That Regulates Ingestion by Integrating Food and Hunger Signals." *Cell* 165 (3): 715–29. doi:10.1016/j.cell.2016.02.061.
Yu, Jai Y., Makoto I. Kanai, Ebru Demir, G. S X E Jefferis, and Barry J. Dickson. 2010. "Cellular Organization of the Neural Circuit That Drives Drosophila Courtship Behavior." *Current Biology* 20 (18): 1602–14. doi:10.1016/j.cub.2010.08.025.
Zhang, Yong Q, Christopher K Rodesch, and Kendal Broadie. 2002. "Living Synaptic Vesicle Marker: Synaptotagmin-GFP." *Genesis* 34 (1-2): 142–45. doi:10.1002/gene.10144.
Zhou, Chuan, Romain Franconville, Alexander G. Vaughan, Carmen C. Robinett, Vivek Jayaraman, and Bruce S. Baker. 2015. "Central Neural Circuitry Mediating Courtship Song Perception in Male Drosophila." *eLife* 4 (September 2015). doi:10.7554/eLife.08477.
Zhou, Chuan, Yufeng Pan, Carmen C. Robinett, Geoffrey W. Meissner, and Bruce S. Baker. 2014. "Central Brain Neurons Expressing Doublesex Regulate Female Receptivity in Drosophila." *Neuron* 83 (1): 149–63. doi:10.1016/j.neuron.2014.05.038.